Crystallization Studies of 5'-deoxyadenosyl Radical Enzymes

By
Laura Phillips

B.A. Chemistry
Carleton College

Submitted to the Department of Chemistry in September 2007 in Partial
Fulfillment of the Requirements for the Degree of

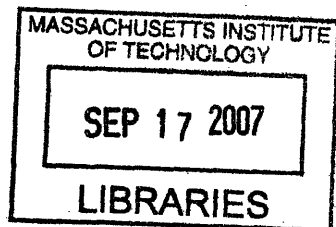Master of Science
in Biological Chemistry

At the

Massachusetts Institute of Technology
September 2007

© 2007 Massachusetts Institute of Technology

Signature of Author_____

Department of Chemistry
August 2007

Certified by_____

Catherine L. Drennan
Associate Professor
Thesis supervisor

Accepted by_____

Robert W. Field
Chairman, Departmental Committee on Graduate Students

Crystallization Studies of 5'-deoxyadenosyl Radical Enzymes

By

Laura Phillips

Submitted to the Department of Chemistry in September 2007 in Partial Fulfillment of
the Requirements for the Degree of Master of Science in Biological Chemistry

ABSTRACT

Both adenosylcobalamin- and S-adenosylmethionine-dependent radical enzymes use a 5'-deoxyadenosyl radical intermediate to abstract a hydrogen atom from their substrates. In the case of adenosylcobalamin-dependent enzymes, the 5'-deoxyadenosyl radical is generated by homolytic cleavage of the carbon-cobalt bond of adenosylcobalamin. In the case of S-adenosylmethionine-dependent radical enzymes, the 5'-deoxyadenosyl radical is generated by reductive cleavage of the S-adenosylmethionine following injection of an electron into the sulfur atom by a reduced [4Fe-4S] cluster. Most known structures of adenosylcobalamin- and S-adenosylmethionine-dependent radical enzymes show that the enzyme active site is in a full or partial TIM barrel. In order to further understanding of the catalytic requirements of enzymes in these classes, crystallization studies were undertaken on four enzymes. The structure of the resting form of lysine 5,6-aminomutase, an adenosylcobalamin-dependent enzyme, is known from previous work in our laboratory; however, the structure of a catalytic state has not been solved. Here, crystallization experiments were performed to try to trap the catalytic enzyme form. Human adenosyltransferase catalyzes the formation of adenosylcobalamin from cob(II)alamin and adenosine triphosphate. Crystallization experiments were set up with and without cobalamin to try to solve its structure. Lipoate synthase is another S-adenosylmethionine-dependent radical enzyme, performing two sulfur insertion reactions on a protein-bound octanoyl group to form a lipoyl group. Crystallization experiments were performed on this enzyme, with and without the substrate, in an attempt to solve its structure and better understand the mechanism of sulfur insertion. Class III ribonucleotide reductase activase is an S-adenosylmethionine-dependent radical enzyme that activates class III ribonucleotide reductase by abstracting a hydrogen atom from a glycine residue. Crystallization experiments were performed with both enzymes present in order to try to determine the structure of the complex; the activase is unstable alone. Thus far, none of the crystallization experiments described here resulted in crystals of high enough quality to solve the structures of these enzymes.

Thesis supervisor: Catherine Drennan
Title: Associate Professor

Acknowledgements

First, thank you to Professor Cathy Drennan for all of her help, support, and advice, on topics ranging from my next experiment to my future plans.

Thanks to the Drennan lab members for always being willing to take the time to answer my questions—and for making lab work fun! Thanks to Leah, Christine, and Yan, for always being in my corner—both literally and figuratively.

Thanks to the Licht and Klibanov lab students for all of the great conversations in the lunchroom!

Thanks to Sarah for calling whenever I needed non-scientific intellectual stimulation—or just a funny story.

Finally, thanks to my family for living up to their reputation as "the best of the families."

Table of Contents

3. Lipoate synthase and class III ribonucleotide reductase activating enzyme crystallization studies

List of Abbreviations

Ado•	5'-deoxyadenosyl radical
AdoCbl	Adenosylcobalamin
AdoMet	Adenosylmethionine
BioB	Biotin synthase
DMB	Dimethylbenzimidazole
2,3-LAM	Lysine 2,3-aminomutase
5,6-LAM	Lysine 5,6-aminomutase
LipA	Lipoate synthase
MCM	Methylmalonyl-CoA mutase
PLP	Pyridoxal 5'-phosphate
RNR	Ribonucleotide reductase
TPP	Thiamine pyrophosphate

1. Introduction

1.1. Radical enzymology

Radical enzymes are critical for cell function, often catalyzing the most challenging of enzymatic reactions. In the last 15 years, knowledge of enzymatic reactions that employ radical intermediates to catalyze difficult chemistry has increased dramatically *(reviewed in 1)*. Organic radical mechanisms are used in areas as diverse as isomerization, DNA synthesis and repair, vitamin synthesis, and antibiotic synthesis. Radical reactions employ coenzymes to generate or stabilize the radical. Some of the same coenzymes commonly used in two-electron enzymatic reactions, such as pyridoxal 5'-phosphate (PLP), thiamine pyrophosphate (TPP), and adenosylmethionine (AdoMet), can also facilitate radical reactions. Metallocofactors can facilitate radical generation by taking advantage of the redox characteristics of metals. Two mechanisms that are commonly used to abstract a hydrogen atom from a substrate without the use of molecular oxygen are discussed here. The first involves homolytic cleavage of AdoCbl to generate the 5'-deoxyadenosyl radical (Ado•); the second uses a 4Fe-4S cluster and AdoMet to generate Ado•.

1.2. Adenosylcobalamin-dependent enzymes

AdoCbl-dependent enzymes are found in organisms ranging from bacterial species to humans. AdoCbl is used by enzymes to catalyze several types of reactions including 1,2 rearrangements in which a group attached to a carbon atom is interchanged with a hydrogen atom on the adjacent carbon *(2)*. The cofactor contains an organometallic bond between carbon 5 on the ribose portion of the adenosyl group and the cobalt, which is

coordinated by the nitrogen atoms in the corrin ring and the dimethylbenzimidazole (DMB) (Figure 1.1). The cofactor can bind either "base-on," with the DMB coordinating the cobalt as the lower ligand, or "base-off," with the DMB displaced by a histidine residue from the enzyme as the lower ligand.

1.2.1. General mechanism

Catalysis is initiated by homolytic cleavage of the weak (~30 kcal/mol *(3)*) C-Co bond, creating cob(II)alamin and Ado•. Since AdoCbl is a highly reactive cofactor, organisms must prevent it from generating uncontrolled radicals; homolysis is usually triggered by substrate binding. Ado• is highly reactive, and quickly abstracts a hydrogen atom from the substrate. In B_{12}-dependent isomerases, this substrate radical can undergo a rearrangement to form a product radical and then back-abstract a hydrogen atom from the deoxyadenosine to re-create Ado•, which can then re-combine with cob(II)alamin to re-form the cofactor (Figure 1.2).

1.2.2. Reactions catalyzed by adenosylcobalamin-dependent enzymes

AdoCbl enzymes catalyze a variety of reactions. All of the isomerases catalyze a 1,2 rearrangement between a hydrogen atom and a substituent that can be oxygen, nitrogen, or carbon. In diol dehydratase and glycerol dehydratase, the migrating group is an –OH, which moves to a carbon that already has an –OH substituent, and water is eliminated (Figure 1.3). In Lysine 5,6-aminomutase (5,6-LAM), ornithine aminomutase, and ethanolamine ammonia lyase, an –NH$_2$ group migrates (Figure 1.3); in ethanolamine ammonia lyase, ammonia is eliminated in a mechanism similar to that of diol

dehydratase. In glutatmate mutase and methylmalonyl-CoA mutase (MCM), a carbon skeleton rearrangement occurs via migration of a carbon substituent (Figure 1.3). In class II ribonucleotide reductase (class II RNR), another AdoCbl-dependent enzyme, AdoCbl is used in a reduction reaction mediated by a thiyl radical formed by hydrogen abstraction from a cysteine thiol, which then catalyzes the reduction of ribonucleotides (Figure 1.3). While the overall mechanism of this reaction varies greatly from that of the isomerases, in every case, the reaction involves abstraction of a hydrogen atom by Ado•.

1.2.3. Adenosylcobalamin transport and activation

For AdoCbl-dependent isomerases in the absence of substrate, the cobalamin homolysis products are not observable in solution; however, upon substrate binding, the homolytic cleavage rate is increased a trillionfold *(4)*. An important question in the study of AdoCbl enzymes is how the enzyme avoids generating potentially harmful radicals in the absence of substrate, and how the substrate binding increases the cleavage rate so dramatically. In addition, the organism must avoid generating radicals from AdoCbl before it is loaded on the enzyme. This is important both in protecting the cell from radical damage and protecting the cofactor from destruction, since cobalamin biosynthesis requires a lot of energy. The cobalamin transport system in humans has been studied extensively, and it appears as though cobalamin is essentially always protein-bound in the body *(5)*.

While many different AdoCbl isomerases are found in bacteria, humans use AdoCbl in only one enzyme, MCM, which performs a carbon skeleton rearrangement to convert

methylmalonyl-CoA into succinyl-CoA. If this enzyme is inactive, methylmalonic aciduria, a potentially fatal condition, can result. It has been suggested that human adenosyltransferase (hATR) both catalyzes the reaction that forms AdoCbl from cobalamin and adenosine 5'-triphosphate (ATP) and acts as a chaperone, handing off AdoCbl to MCM (6). This delivery service would prevent side reactions that could occur if the AdoCbl was floating around in the cell. Once the AdoCbl is in place on the enzyme, it is also necessary to control reactivity to prevent radical damage to the enzyme. In the case of MCM, this is achieved in part through the coupling of substrate binding to C-Co bond homolysis (7), and in part through protection of the enzyme by MeaB, a chaperone that binds to MCM and prevents inactivation (8).

1.3. Adenosylmethionine radical enzymes

AdoMet has long been known as a methylating agent used in many pathways in the cell (reviewed in 9). More recently, enzymes that use AdoMet as a free radical initiator have been characterized (reviewed in 1). AdoMet radical enzymes participate in biosynthetic and catabolic pathways and are present in all three kingdoms of life. All AdoMet radical enzymes contain a CxxxCxxC motif, with the three cysteines coordinating three of the irons in the [4Fe-4S] cluster (10). The fourth iron of the [4Fe-4S] cluster is coordinated by AdoMet itself, by its amino group and carboxylate oxygen (11).

1.3.1. General mechanism

The cluster must be reduced from its resting state of $[4Fe-4S]^{2+}$ to $[4Fe-4S]^{1+}$ for activity; in E. coli, this reduction is catalyzed by flavodoxin (12). The reduced cluster transfers an

electron to AdoMet, reductively cleaving the carbon-sulfur bond to produce methionine and Ado•, while simultaneously regenerating the [4Fe-4S]$^{2+}$ cluster (Figure 1.4). The carbon-sulfur bond cannot be cleaved homolytically as in AdoCbl-dependent enzymes because the bond is too strong (greater than 60 kcal/mol) *(13)*. After cleavage, the 5'-deoxyadenoxyl radical abstracts a hydrogen atom from the substrate. After the reaction occurs, in some cases (lysine 2,3-aminomutase (2,3-LAM), spore photoproduct lyase), the AdoMet is re-formed *(1)*; in other cases (lipoate synthase (LipA), class III RNR, Biotin Synthase (BioB)), methionine and 5'-deoxyadenosine are products of the reaction *(1)*.

1.3.2. Reactions catalyzed by AdoMet radical enzymes

AdoMet radical enzymes catalyze reactions on a huge variety of substrates, ranging from as small as the single amino acid lysine to large proteins (Figure 1.5). These reactions include amino group migration, carbon-carbon bond cleavage, carbon-sulfur bond formation, alcohol oxidation, and glycyl radical formation. While the substrates vary greatly in size and the reactions vary greatly in outcome, all are initiated by the abstraction of a hydrogen atom. In the class III RNR activating enzyme and pyruvate formate lyase activating enzyme, as well as other enzymes, the AdoMet radical enzyme abstracts a hydrogen atom from a glycine residue in another protein; this glycyl radical then goes on to catalyze another reaction. In the case of class III RNR, this glycyl radical abstracts a hydrogen atom from a cysteine, forming the thiyl radical necessary for ribonucleotide reduction with a similar mechanism to the other classes of RNR.

1.4. Adenosyl radical chemistry and enzymology

AdoMet radical enzymes use a [4Fe-4S] cluster and AdoMet to create Ado•, while adenosylcobalamin (AdoCbl)-dependent isomerases also generate Ado• using coenzyme B_{12}. Both AdoMet radical enzymes and AdoCbl isomerases can have TIM barrel folds or partial TIM barrel folds where the radical chemistry occurs *(14)*. TIM barrels were first discovered in the enzyme triose phosphate isomerase and are ubiquitous in nature. They are most often involved in energy metabolism, but are present in at least 28 different enzyme classes. A full TIM barrel consists of an $(\alpha\beta)_8$ motif. The β-sheets line the interior of the barrel, which can protect reactive intermediates from solvent. While in the solved structures of AdoCbl enzymes, the TIM barrel is the full $(\alpha\beta)_8$ barrel *(15, 16, 17, 18, 19, 20)*, three out of the four structures of AdoMet radical enzymes have a three-quarters $(\alpha\beta)_6$ barrel *(21, 22, 23, 24)*. Superposition of the TIM barrel of AdoCbl-dependent diol dehydratase with that of the AdoMet radical enzyme BioB shows that the ring of diol dehydratase's AdoCbl occupies the same position as the [4Fe-4S] cluster in BioB *(14)*.

The AdoMet and AdoCbl cofactors are related solely by the 5'-deoxyadenosyl moiety present in both compounds (Figure 1.1). Since both AdoMet radical enzymes and AdoCbl isomerases use the same putative radical intermediate, they can catalyze very similar reactions. 2,3-LAM and 5,6-LAM perform essentially the same chemistry in the same pathway, yet 2,3-LAM is a AdoMet radical protein and 5,6-LAM is AdoCbl-dependent. After the generation of Ado•, the proposed mechanisms are the same. Both

enzymes use PLP to bind the lysine and potentially to stabilize the radical intermediates *(13, 25)*. Why would nature choose to catalyze 1,2 amino migrations with different sources of Ado•? Similarly, class II RNR uses AdoCbl to form the thiyl radical, whereas class III RNR activase is an AdoMet radical enzyme that creates the thiyl radical via a glycyl radical intermediate. The structures of these enzymes would be very interesting to compare in order to see the requirements for AdoCbl catalysis vs. AdoMet catalysis.

1.5. Summary

AdoMet and AdoCbl radical enzymes catalyze important reactions via an Ado• intermediate. AdoMet-dependent enzymes use a [4Fe-4S] cluster and a reducing system to reductively cleave the AdoMet, creating the radical. In AdoCbl-dependent enzymes, the carbon-cobalt bond of the AdoCbl is homolytically cleaved to create the same radical species. Both the AdoMet radical enzymes and the AdoCbl isomerases use a TIM barrel fold or partial TIM barrel fold to sequester radical intermediates. Given these similarities, it is not surprising that these classes of enzymes can catalyze very similar reactions.

I have worked on four projects in the AdoMet and AdoCbl enzyme families. I have performed crystallization trials of 5,6-LAM, an AdoCbl isomerase (Chapter 2), and hATR, an adenosyltransferase that transfers the adenosyl group onto cobalamin in humans (Chapter 2). I have also worked on NrdG, the class III RNR activase (Chapter 3), and LipA, a sulfur insertion enzyme (Chapter 3); both are AdoMet radical enzymes.

1.6. Figures

A   B   C
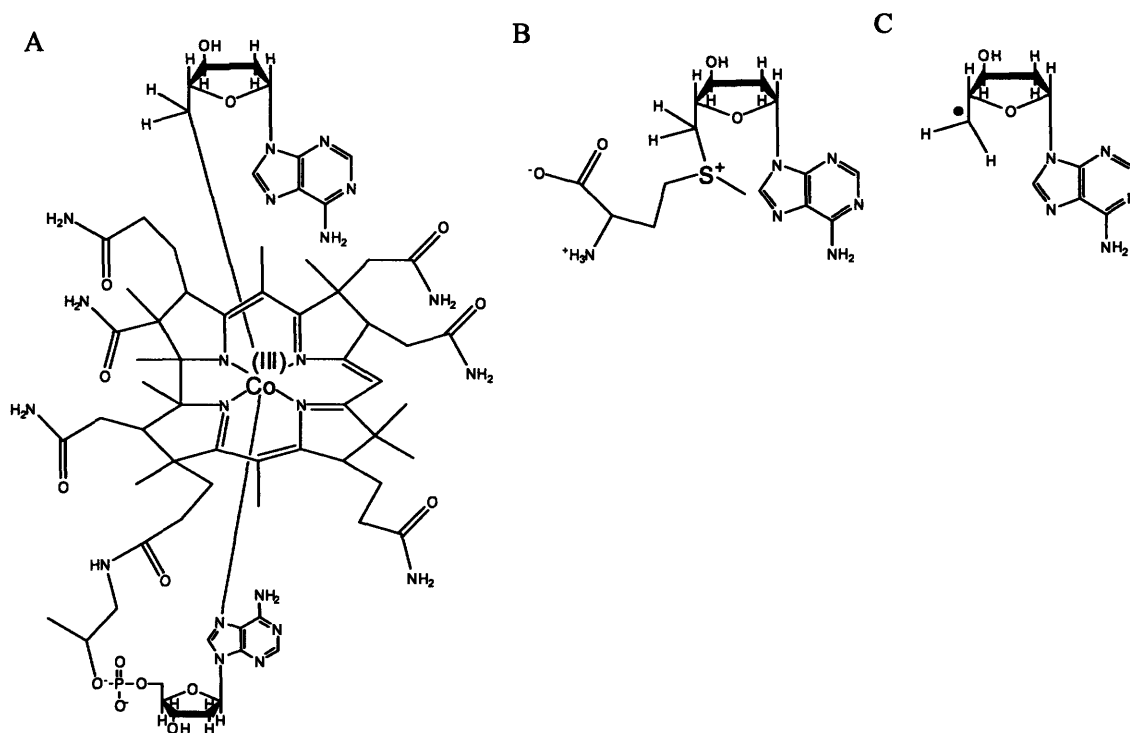
Figure 1.1. A. Structure of AdoCbl (coenzyme B_{12}). B. Structure of AdoMet. C. Structure of Ado•.
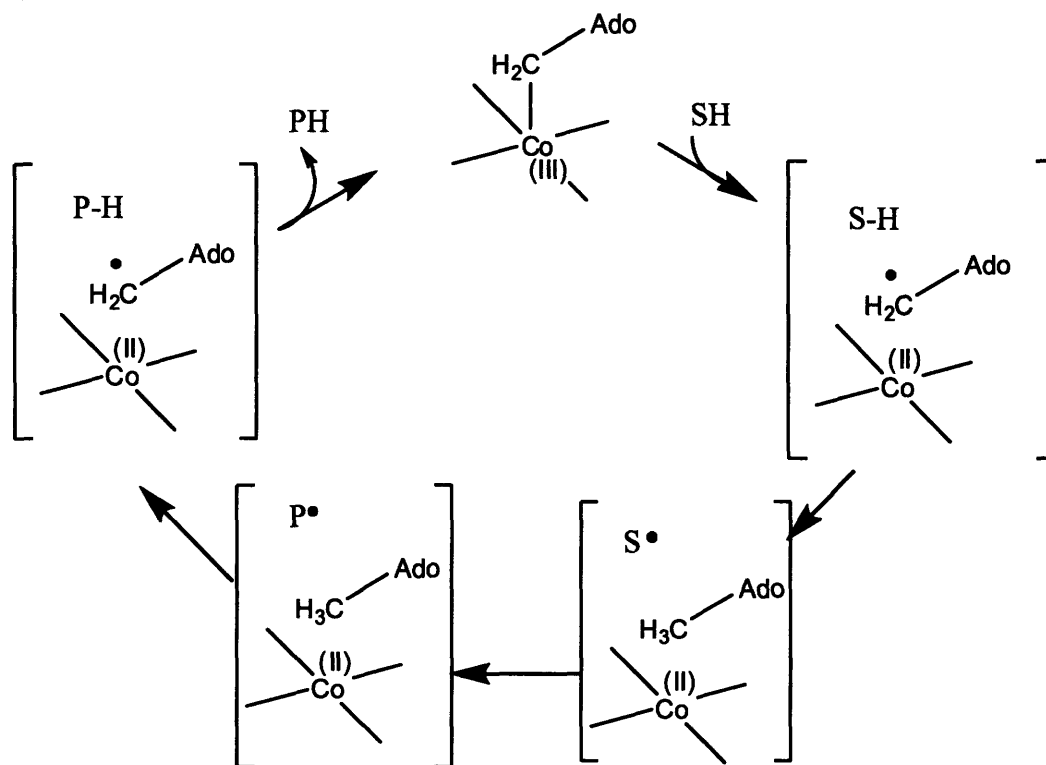
Figure 1.2. General reaction mechanism for AdoCbl-dependent isomerases.

14
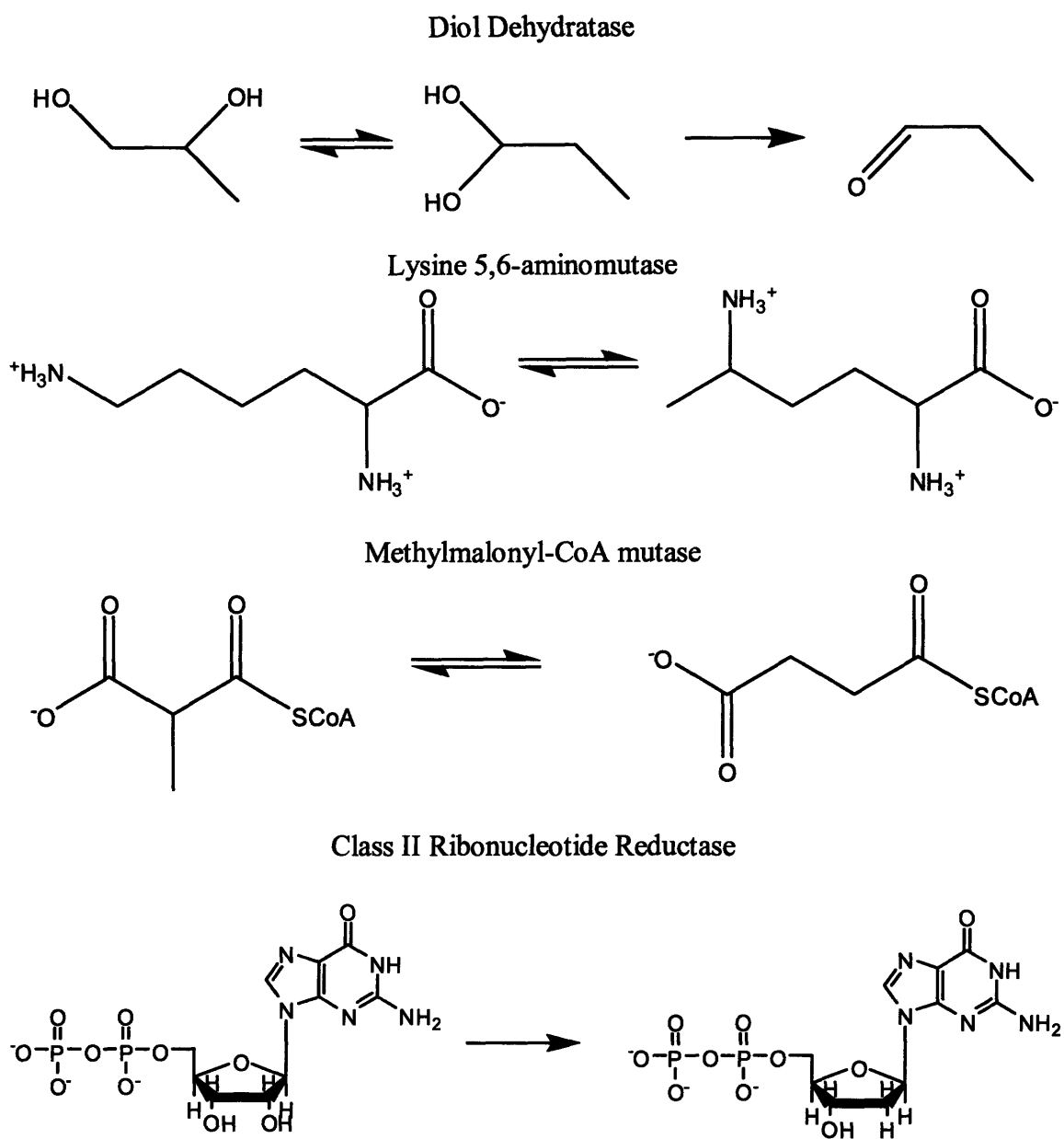
Figure 1.3. Examples of reactions catalyzed by AdoCbl-dependent enzymes.
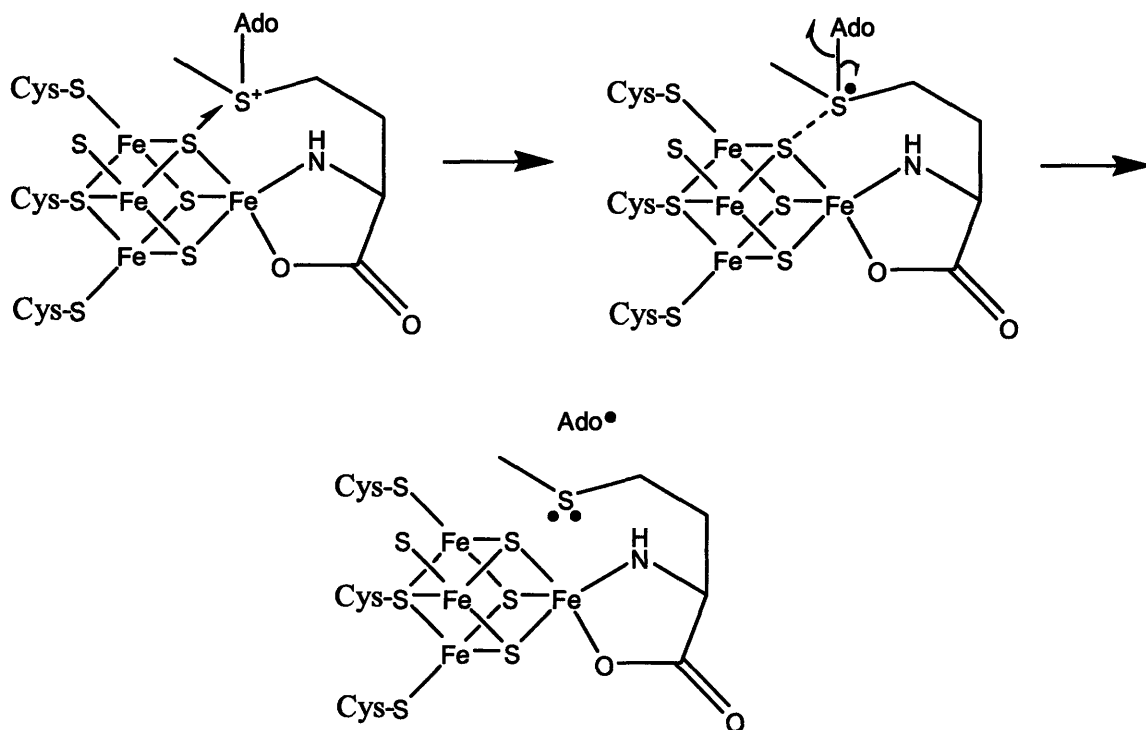
Figure 1.4. Possible mechanism of Ado• radical formation. Electron transfer from the Fe₄S₄ cluster to the AdoMet could result in the formation of a transient sulfonium radical species. The cleavage of the C-S bond of AdoMet would then lead to the formation of Ado• and Met.

Lysine 2,3-aminomutase
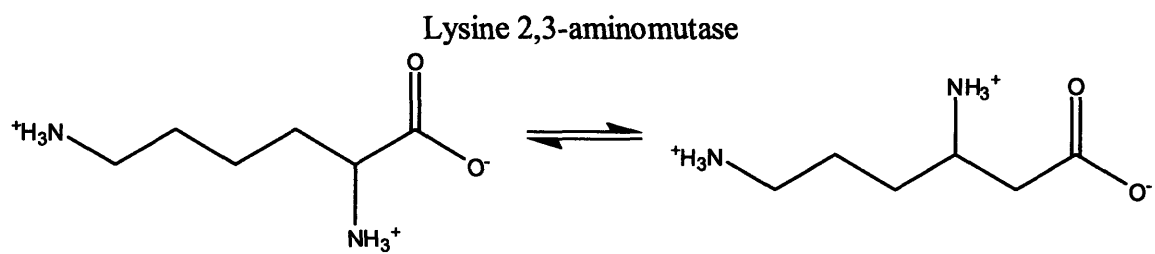
Class III ribonucleotide reductase activase and Pyruvate formate lyase activase
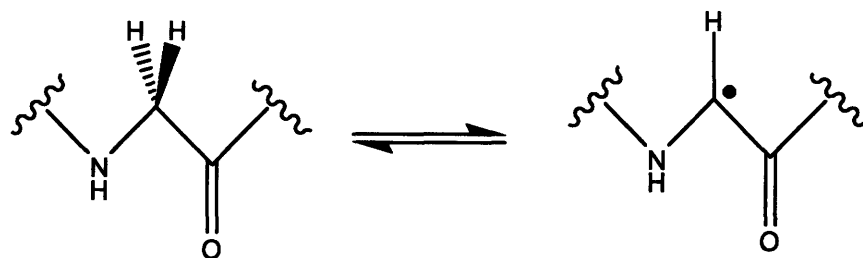
Biotin Synthase
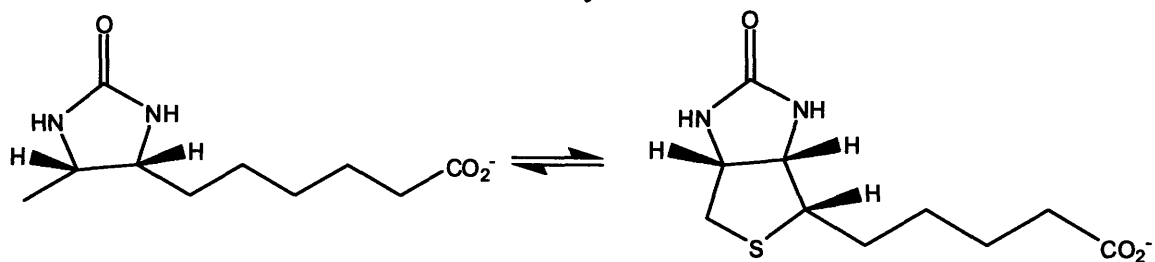
Lipoate Synthase
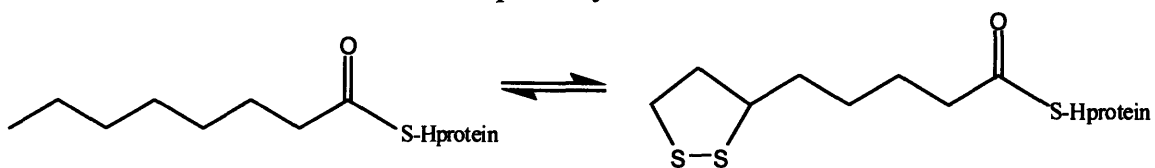
Figure 1.5. Examples of reactions catalyzed by AdoMet radical enzymes.

1.7. References

1. Frey PA. (2001) *Annual Review of Biochemistry* 70, 121-148.
2. Banerjee R and Ragsdale SW. (2003) *Annu. Rev. Biochem.* 72, 209-247.
3. Finke RG and Hay BP. (1984). *Inorg Chem.* 23, 3041-3043.
4. Lang D, Thoma R, Henn-Sax M, Sterner R, and Wilmanns M. (2000) *Science* 289, 1546-50.
5. Banerjee R. (2006) *ACS Chem Biol.* 1, 149-159.
6. Yamanishi M., *et. al.* (2005) *TRENDS in Biochem. Sci.* 30, 304-308.
7. Mancia. F., Smith, G.A., Evans, P.R. (1999) *Biochemistry* 25, 7999-8005.
8. Korotkova N, Lidstrom ME. (2004) *J Biol Chem.* 279, 13652-8.
9. Loenen WA. (2006) *Biochem Soc Trans.* 34, 300-303.
10. Sofia HJ, Chen H, Hetzler BG, Reyes-Spindola JF, and Miller N. (2001) *Nucleic Acids Res.* 29, 1097-1106.
11. Buis JM and Broderick JB. (2005) *Arch Biochem Biophys.* 433, 288-96.
12. Mulliez E, Padovani D, Atta M, Alcouffe C, and Fontecave M (2001) *Biochemistry.* 40, 3730-6.
13. Frey PA and Reed GH. (2000) *Arch Biochem Biophys.* 382, 6-14.
14. Nicolet Y and Drennan C. (2004) *Nucleic Acids Res* 32, 4015-4025.
15. Sintchak MD, Arjara G, Kellogg BA, Stubbe J, and Drennan CL. (2002) *Nat Struct Biol.* 9, 293-300.
16. Berkovitch F, Behshad E, Tang KH, Enns EA, Frey PA, and Drennan CL. (2004) *Proc Natl Acad Sci.* 101, 15870-15875.
17. Reitzer R, Gruber K, Jogl G, Wagner UG, Bothe H, Buckel W, and Kratky G. (1999) *Structure* 7, 891-902.
18. Mancia F, Keep NH, Nakagawa A, Leadlay PF, McSweeney S, Rasmussen B, Bosecke P, Diat O, and Evans PR. (1996) *Structure* 4, 339-350.
19. Liao DI, Dotson G, Turner I Jr, Reiss L, and Emptage M. (2003) *J Inorg Biochem.* 93, 84-91
20. Shibata N, Masuda J, Tobimatsu T, Toraya T, Suto K, Morimoto Y, and Yasuoka N. (1999) *Structure.* 7, 997-1008.
21. Berkovitch F, Nicolet Y, Wan JT, Jarrett JT, and Drennan CL. (2004) *Science* 303, 76-79.
22. Hanzelmann P, Schindelin H. (2004) *Proc Natl Acad Sci.* 101, 12870-5.
23. Layer G, Moser J, Heinz DW, Jahn D, and Schubert WD. (2003) *EMBO J.* 22, 6214-24.
24. Lepore BW, Ruzicka FJ, Frey PA, and Ringe D. (2005) *Proc Natl Acad Sci* 102, 13819-24.
25. Wetmore SD, Smith DM, and Radom L. (2004) *J. Am. Chem. Soc.* 123, 8678-8689.

2. Lysine 5,6-aminomutase and human adenosyltransferase crystallization studies

2.1. Introduction to crystallography with adenosylcobalamin

To date, the structures of several adenosylcobalamin (AdoCbl)-dependent enzymes have been solved (1,2,3,4,5,6,7). Aside from class II ribonucleotide reductase (RNR), which has a structure more like that of the RNR family than that of other AdoCbl-dependent enzymes (1), all of these enzymes employ a TIM barrel as their catalytic subunit. The structure of the AdoCbl-binding domain differs according to cobalamin binding mode. The structures where AdoCbl is bound base-off contain a Rossmann-like fold, with AdoCbl bound near the C-terminus of this domain (2,3,4). In contrast, in the structures and predicted structures where AdoCbl is bound base-on, the cofactor is bound on the edge of a beta sheet near the C-terminus of the protein (5,6,7). Given the weakness of the carbon-cobalt bond, it is unsurprising that the X-ray beam often cleaves the cofactor, and in some cases the upper ligand is not seen at all in the structure (4). Interestingly, a very long lower ligand nitrogen-cobalt bond has been seen in many of the structures (3,4); however, this could be due to X-ray beam reduction of the cobalt instead of bond lengthening upon cobalamin-enzyme interaction.

2.2. Lysine 5,6-aminomutase

2.2.1. Introduction to lysine 5,6-aminomutase

AdoCbl-dependent isomerases catalyze 1,2 rearrangements of a function group (or carbon) and a hydrogen atom. These enzymes are often found in catabolic pathways, rearranging the functional group or carbon skeleton to allow further degradation of the product. Lysine 5,6-aminomutase (5,6-LAM), an AdoCbl and pyridoxal 5'-phosphate

(PLP)-dependent enzyme, catalyzes the radical-based 1,2 amino migration of the ϵ amino group from carbon 6 to carbon 5 of DL-lysine and L-β-lysine (Figure 2.1). Lysine 2,3-aminomutase (2,3-LAM), also part of the lysine fermentation pathway, catalyzes the interconversion of lysine and L-β-lysine (Figure 2.1), but uses an AdoMet radical mechanism. In 5,6-LAM, turnover is initiated upon substrate binding through homolysis of the C-Co bond of AdoCbl to form Ado• (Figure 2.2). As with the other isomerases, there is a large acceleration of C-Co bond homolysis upon substrate binding.

The role of PLP in the isomerization is not clear. It has been postulated that the role of PLP is to stabilize radical intermediates with its conjugated pi system, a hypothesis that has been supported by computational studies (8). However, a simple model for the 5,6-LAM reaction, the rearrangement of the aziridylcarbinyl radical, occurs without an aromatic substituent at cryogenic temperatures (9). The latter suggests that the rearrangement catalyzed by 5,6-LAM could occur without PLP. Interestingly, 2,3-LAM also has PLP as a cofactor (10), suggesting that PLP has mechanistic relevance.

2.2.2. Previous work in the Frey laboratory

While 5,6-LAM had been previously identified, the development of an *E. coli* expression and purification system in the Frey lab at the University of Wisconsin facilitated further studies (11). The recombinant protein is six times as active as protein isolated from *C. sticklandii* (11). The base-off binding of AdoCbl was confirmed by EPR (11). Through EPR and UV/Vis spectroscopy, the abstraction of a hydrogen atom from C5 of lysine was found to be the rate-limiting step of the reaction (12).

The Frey lab also studied the inactivation of the enzyme. 5,6-LAM is inactivated rapidly in the absence of the E2 activating enzyme and ATP. E2 uses ATP to re-activate 5,6-LAM, but the mechanism of the reactivation is unknown *(13)*. The inactivation occurs at the same rate as production of 5'-deoxyadenosine and cob(III)alamin *(14)*. Tang, Chang, and Frey proposed that this inactivation is likely caused by an electron transfer from cob(II)alamin to the substrate or product radical followed by a proton transfer to the newly formed carbanion, creating either substrate or product, 5'-deoxyadenosine, and cob(III)alamin *(14)*. This inactivation happens more rapidly when beta lysine is the substrate *(14)*.

2.2.3. Structure of lysine 5,6-aminomutase in the "resting" conformation

The crystal structure of the substrate-free form of 5,6-LAM was solved to 2.8 Å resolution in our laboratory by Fred Berkovitch *(1)*. The structural analysis reveals that 5,6-LAM uses the same structural motifs as several other AdoCbl-dependent enzymes: a Rossmann-like domain for binding the AdoCbl with a histidine coordinating the cobalt instead of the DMB, and an $(\alpha\beta)_8$ TIM domain for housing the active site (Figure 2.2). PLP, not a cofactor in the other AdoCbl-dependent enzymes with known structures, sits at the top of the TIM barrel, in the putative active site (Figure 2.3). The orientation of the Rossmann and TIM barrel domains with respect to each other is not the same as in other AdoCbl-dependent enzymes. In MCM and glutamate mutase, the structures also contain a Rossmann domain and a TIM barrel, but the AdoCbl is positioned over the TIM barrel, already in the active site. The TIM barrel shields the active site, keeping radical

intermediates safely inside. In 5,6-LAM, a novel linkage between PLP and Lys[144] of the Rossmann domain enforces an alternate conformation that positions the AdoCbl cofactor 25 Å away from the active site (Figure 2.4A). The covalent linkage between the Rossmann domain and PLP effectively locks 5,6-LAM into a non-catalytic configuration until substrate binds and releases Lys[144] via a transaldimination reaction. The Rossmann domain, now untethered to the PLP, could rotate, moving the AdoCbl into the active site, positioning it at the top of the TIM barrel. Hydrogen abstraction from carbon 5 of the substrate lysine, the first step in the rearrangement, could then occur (Figure 2.2). This mechanism would represent a novel means of coupling substrate binding to conformational change through the use of PLP in an AdoCbl dependent enzyme, preventing radical damage to the enzyme.

2.2.4. Crystallization experiments

In order to confirm the above mechanism and explore the molecular details of the signaling mechanism and conformational change, crystallization experiments were performed on a K144βA mutant of 5,6-LAM, obtained from the Frey laboratory (Table 2.1). This mutant turns over very slowly (Elham Beshad, Personal Communication). Without the lysine to lock the AdoCbl-Rossmann domain in the resting state, AdoCbl-Rossmann domain should assume the catalytic position over the TIM barrel (similar to Figure 2.3B).

Using the hanging-drop vapor diffusion method, preliminary microcrystals were obtained with a hit from the Hampton Index screen at room temperature (15 mg/mL protein in 5.8

mM triethanolamine, pH 7.8, 1 μL:1 μL drops over 500 μL well solution with 0.2 M ammonium acetate, 0.1 M Tris pH 8.5, 25% w/v PEG 3350) (Figure 2.4C). These crystallization conditions were screened around, varying salt, buffer, and precipitant, and slightly larger crystals (~30 μm) were obtained with an optimized condition (0.2 M ammonium acetate, 0.1 M HEPES pH 8.2, 25% w/v PEG 2000 monomethylether). These crystals took approximately 4 weeks to grow. To improve these crystals, microseeding was performed by crushing up crystals and pipetting serial dilutions of these crushed crystals into drops that had been equilibrating for one day. Through this technique, slightly larger (40 μm) crystals (Figure 2.5 C) were grown, but there was no diffraction in the X-ray beam at room temperature or in the cryostream. Detergent and additive screens were performed; however, the crystals grown in the additive and detergent screens did not show any improvement over the original crystals.

In addition to the mutant form of LAM, crystallization screens were performed with the wild type enzyme with either lysine or ornithine bound, with the hope of trapping the protein in the catalytic "on" form (Table 2.2). Ornithine binds well to 5,6-LAM, and can be used as an inhibitor. It does not appear to turn over, but, like lysine, it can initiate C-Co bond cleavage and form an inactivated complex where an electron is likely transferred from cob(II)alamin to the organic radical on the substrate or product, forming cob(III)alamin and a carbanion, which would be quickly protonated to form 5'-deoxyadenosine (Elham Beshad, Personal Communication).

Preliminary crystals were grown in one of the Hampton Index screen conditions at room temperature (wild-type protein at 12 mg/mL, 0.5 mM 2-mercaptoethanol, 10 mM triethanolamine, pH 7.2, 5mM ornithine, 1 μL:1 μL drops over a 500 μL well solution with 22% polyacrylic acid, 0.1 M HEPES pH 7.5, 0.02 M MgCl$_2$) using the Hanging-drop diffusion method (Figure 2.5A). These crystals were very small, and optimization yielded little improvement with the first protein sample used. The second protein preparation obtained from the Frey laboratory (14 mg/mL in 10 mM triethanolamine pH 8, 0.5 mM BME, 2.5% glycerol) produced much larger (50 μm) crystals of the wild-type enzyme with 5 mM ornithine in the same condition as before (Figure 2.5B).

Crystals were cryoprotected with 20% ethylene glycol and 20% glycerol solutions that included the mother liquour solution components at original concentrations. These crystals did not show any diffraction on our home X-ray equipment. However, crystals were sent to the synchrotron at Stanford to determine if any diffraction could be seen using a more intense X-ray beam. At the home beam, no ice rings were seen when crystals were cryoprotected, but there were significant ice rings at the synchrotron, perhaps due to problems with crystal storage. At the synchrotron, the ethylene glycol cryoprotected crystal diffracted well to 8 Å, weakly to 4.3 Å (Figure 2.6, 2.7). Indexing the crystal gave a preliminary space group of P3. To improve diffraction, detergent and additive screens were tried. Although crystals grew in these conditions, they still showed no diffraction at home, and it was difficult to reproduce the crystals. It is likely the protein is not amenable to crystallization after a few months of storage.

The poor diffraction could be a result of the Rossmann domain being significantly disordered without AdoCbl bound. Because the presence of both AdoCbl and ornithine can lead to inactivation (Elham Beshad, Personal Communication), crystallization conditions were screened around in the presence of ornithine and cyanocobalaman or hydroxocobalamin. Crystals that appeared to be cyanocobalamin-containing were grown in the same condition as without a cobalamin analog at room temperature (wild-type protein 14 mg/mL in 10 mM triethanolamine pH 8.0, 0.5 mM BME, 2.5% glycerol; 1 μL:1 μL drops over 500 μL well solution with 22% polyacrylic acid, 0.1 M HEPES pH 7.5, 0.02 M MgCl$_2$) with 4.5 mM cyanocobalamin using the Hanging-drop vapor diffusion method. Unfortunately, the resulting crystals are significantly smaller than the crystals without cyanocobalamin (~20 μm), and therefore too small to screen. This condition was optimized somewhat with detergent and additive screens. Upon screening of these optimized crystals, the disperse nature of the reflections in the diffraction pattern showed that these were cyanocobalamin crystals. All crystallization experiments that include cobalamin have been performed in a dark room under red light, and viewed using a microscope with a red filter, in order to avoid cleaving the C-Co bond.

2.2.5. Conclusions and future work

While no 5,6-LAM crystals have diffracted to suitable resolution for structure determination as of yet, there is still a good chance of getting crystals that diffract well. The protein seems to have a short crystallization life; doing frequent protein preparations could potentially make a big difference in crystal reproducibility and quality. In addition, 5,6-LAM from a different organism could be potentially easier to crystallize in the active

conformation. Since other AdoCbl-dependent enzymes have been crystallized in similar conformations *(3,4)*, it should be possible to obtain this structure. If diffraction-quality crystals are obtained, molecular replacement using the TIM barrel of the existing structure should be effective in obtaining phase information. The TIM barrel structure should not change according to our proposed mechanism, making it is a good candidate for molecular replacement.

2.3. Human adenosyltransferase

2.3.1. Introduction to human adenosyltransferase

While the delivery of metal cofactors to their target proteins by chaperones is a recent hot topic (15), relatively little is known about the delivery of highly reactive organic cofactors such as PLP, thiamine pyrophosphate (TPP), and cobalamin. These cofactors are both reactive and present in low concentrations in the cell, making it difficult to get the intact cofactor into the enzyme, both because of cofactor-damaging side reactions and the low probability of the cofactor colliding with its target enzyme in the correct conformation to bind. Chaperone proteins could solve both of these problems, protecting the cofactor from radical damage and delivering the cofactor directly to the target protein in the correct conformation and orientation to bind. From studies performed with [^{57}Co]-cobalamin, it appears that AdoCbl is predominantly protein-bound inside the cell (16).

In humans, cobalamin is a cofactor in only two enzymes: methionine synthase, which uses methylcobalamin, and methylmalonyl-CoA mutase (MCM), which uses AdoCbl. As discussed previously, lack of MCM activity in humans causes a condition known as methylmalonic aciduria, a potentially fatal inborn error of metabolism. Eight complementation groups, cblA-cblH, have been identified that correspond to gene defects associated with intracellular vitamin B$_{12}$ metabolism in humans (17). Three groups, cblA, cblB, and cblH, linked to methylmalonic aciduria, affect steps occurring in the mitochondria, where MCM works. Human adenosyltransferase (hATR), is the locus of mutations in the cblB complementation family (18); several pathogenic mutations in the gene have been identified (19).

In bacteria, there are the PduO, CobA, and EutT families of adenosyltransferases *(20)*. The PduO-type adenosyltransferases are associated with genes that encode AdoCbl-dependent diol dehydratase, glycerol dehydratase, or MCM *(20)*. The CobA family enzymes have been predicted to be important in the assimilation of exogenous cobalamins and the *de novo* biosynthesis of AdoCbl *(21)*. EutT adenosyltransferases are associated with gene clusters that contain AdoCbl-dependent ethanolamine ammonia lyase *(22)*. It has been suggested that each adenosyltransferase might be specific for an AdoCbl-dependent enzyme, supporting the idea of a direct transfer between the adenosyltransferase and the target enzyme *(20)*. It follows that specific protein-protein interactions between the adenosyltransferase and the target protein might be important, making the large number of different adenosyltransferases necessary.

In solution, AdoCbl exists in base-on and base-off conformations; the equilibrium between these two states is governed by the protonation state of the dimethylbenzimidazole (DMB) ligand, with a pK_a of 3.7 *(23)*. When DMB is protonated, it can no longer coordinate the cobalt, and dissociates. Several AdoCbl-dependent isomerases bind the cofactor with the DMB not coordinating the metal, but in these cases DMB is replaced by a histidine ligand from the signature DxHxxG sequence on the cobalamin-dependent enzyme *(24)*. A crystal structure of CobA from *Salmonella typhimurium* has been solved and shows the AdoCbl bound in a base-on conformation *(25)*. The adenosyltransferase with highest sequence homology (32%) to hATR which has been solved is that of a PduO-type enzyme from *Thermoplasma acidophilum;*

unfortunately, the crystal structure does not contain cobalamin, so it is not known how the cofactor is bound (26).

2.3.2. Previous work on human adenosyltransferase in the Banerjee laboratory

AdoCbl is synthesized from cob(II)alamin by an adenosyltransferase and a reductase (27). In humans, the reductase is found in the mitochondria and reduces cob(II)alamin bound to hATR to cob(I)alamin, a supernucleophile, which is then adenosylated by ATP to form AdoCbl (Figure 2.8). The model proposed by Yamanishi, Vlasie, and Banerjee (27), states that the AdoCbl is then transferred by a direct hand-off to MCM. The reduction potential for the cob(II)alamin/cob(I)alamin couple is -610mV in reference to a standard hydrogen electrode, far below that of any in vivo reducing agents (28). Since the cobalamin is bound to hATR during this reduction, hATR must somehow activate cob(II)alamin for this reduction. The UV spectrum of AdoCbl bound to hATR is characteristic of the base-off conformer, with an absorption maximum of 454 nm (29). EPR spectra of cob(II)alamin bound to hATR is also typical of base-off binding (29). Magnetic circular dichroism (MCD) spectra performed by Brunold and co-workers show that cob(II)alamin bound to hATR in the presence of ATP appears to be base-off, with no ligand or a weakly bound water ligand in place of the DMB ligand (30). This coordination could raise the reduction potential by 120mV, allowing the reduction to take place (30). Without ATP bound, the cobalamin appears to be 60% base-on, 40% base-off by MCD (30). Once the cobalamin has been reduced, it is a supernucleophile which attacks C-5 of the ribose portion of ATP, kicking out the triphosphate to form AdoCbl (Figure 2.8).

It is possible that the existence of no lower ligand or a weakly bound water could be important in allowing a direct transfer of AdoCbl from hATR to MCM. The histidine ligand from MCM could perhaps coordinate the Co of AdoCbl, allowing the AdoCbl to then bind MCM in a base-off fashion without the MCM histidine having to directly compete for Co binding with the DMB (Figure 2.9) (27). The binding of AdoCbl is ~40 times tighter in MCM (K_d 0.4 μM) than hATR (K_d 1.7 μM) (29), supporting the idea that a direct hand-off could work efficiently. This hand-off scenario mirrors that seen in metal chaperones and their target proteins (31). A crystal structure of hATR with AdoCbl bound would confirm that this site is open for coordination with the histidine from MCM.

2.3.3. Crystallization experiments

For hATR crystallization, sparse matrix screens have been performed on the apo-protein, the protein with just ATP, with AdoCbl, and with both AdoCbl and ATP (Table 2.3). Small (20 μm) crystals of the apo-protein grew at room temperature (protein 3 mg/mL in 50 mM Tris pH 8.0, 200 mM KCl, 1 μL:1 μL drops over 500 μL well solution with 25% PEG 3350, 0.1 M HEPES pH 7.5, 0.2 M $MgCl_2$) (Figure 2.10A) but no crystals large enough to mount on the X-ray equipment have grown. Precipitant, salt, temperature, and buffer were varied in order to optimize the crystals, but did not have much effect. Slightly larger (~30 μm) crystals were grown by using PEG 2000 monomethyl ether in place of PEG 3350 (Figure 2.10B); unfortunately, these crystals required four weeks to grow, making it time-consuming to further optimize these crystals. No crystals formed in

the conditions with ATP or AdoCbl. All screens set up with AdoCbl (4.5 mM) have been set up in the darkroom under red light, and viewed using a microscope with a red filter.

2.3.4. Crystal structure of hATR solved by Schubert and Hill

While pursuing crystallization of hATR, a paper describing the structure of hATR with ATP bound came out (32). The structure showed a trimeric helical ferritin-like structure, very similar to that of PduO-type cobalamin adenosyltransferases from other species that had been previously solved (Figure 2.11) (32). Since the structure published did not have cobalamin bound, the exact mode of cobalamin binding has not been confirmed, but they modeled in AdoCbl in a base-off conformation with the metal not coordinated by a lower ligand (32).

2.3.5. Conclusions and future work

While this project is not currently being pursued by our laboratory because of the published structure and the lack of crystals with cobalamin bound, it would be ideal to get a structure of hATR with cobalamin bound to confirm the unusual coordination reported by Brunold (30). Schubert and Hill used a mutant with the mitochondrial targeting sequence cut off; screening this mutant with cobalamin bound would be good to try, but has probably already been tried by Schubert and Hill. In addition, a crystal structure was solved of an adenosyltransferase from Lactobacillus reuteri, also with only ATP bound (33); this would also potentially be a good target for crystallization with cobalamin bound.

2.4. Figures
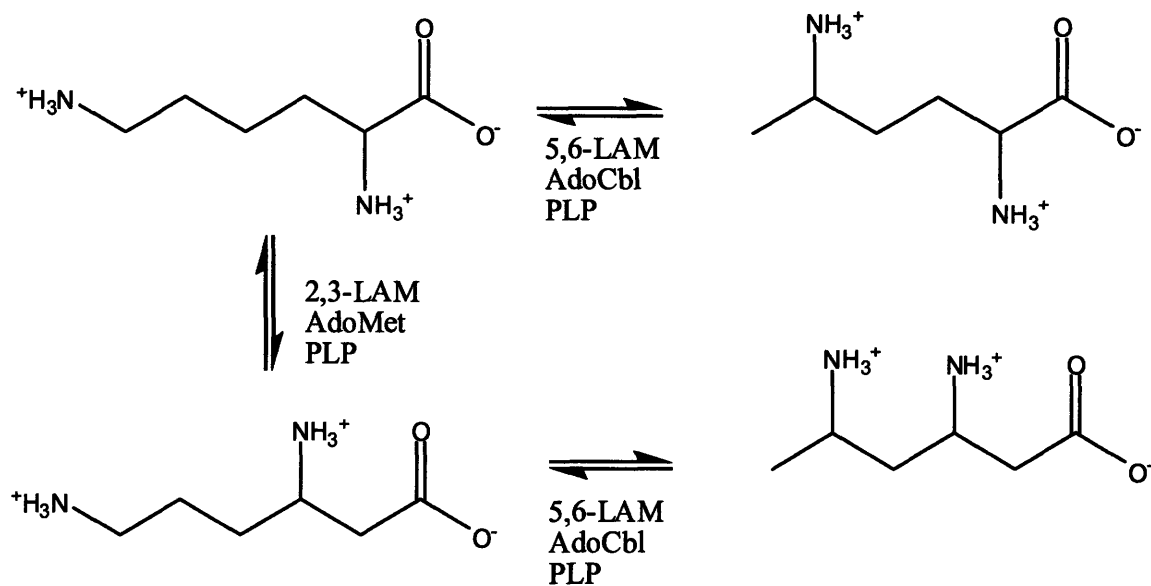
Figure 2.1. A comparison of the reactions catalyzed by 5,6-LAM and 2,3-LAM.
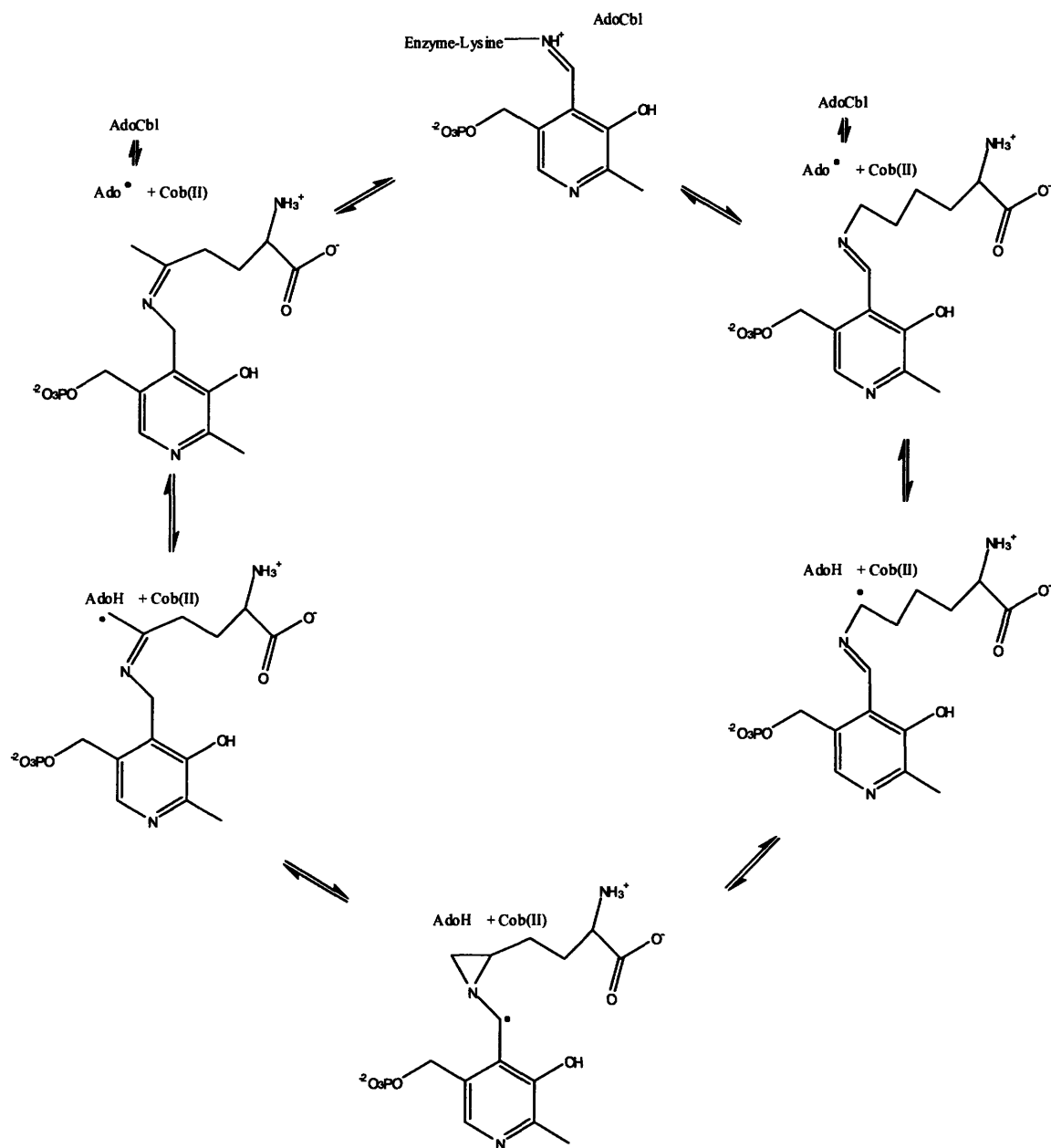
Figure 2.2. The proposed mechanism of 5,6-LAM *(34)*.
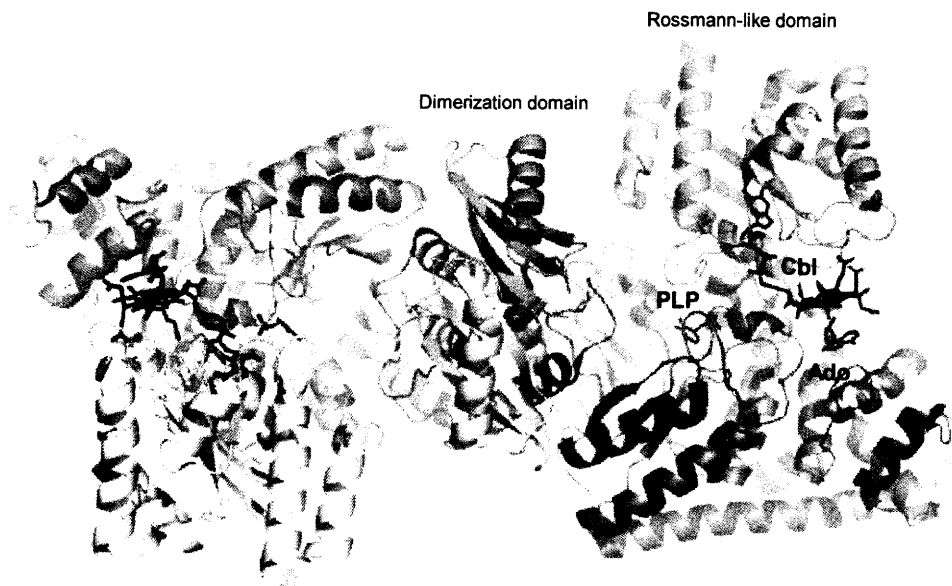
Figure 2.3. Structure of Lysine 5,6 aminomutase, colored by chain. Cbl is represented in red, AdoH in blue, and PLP in magenta *(1)*.
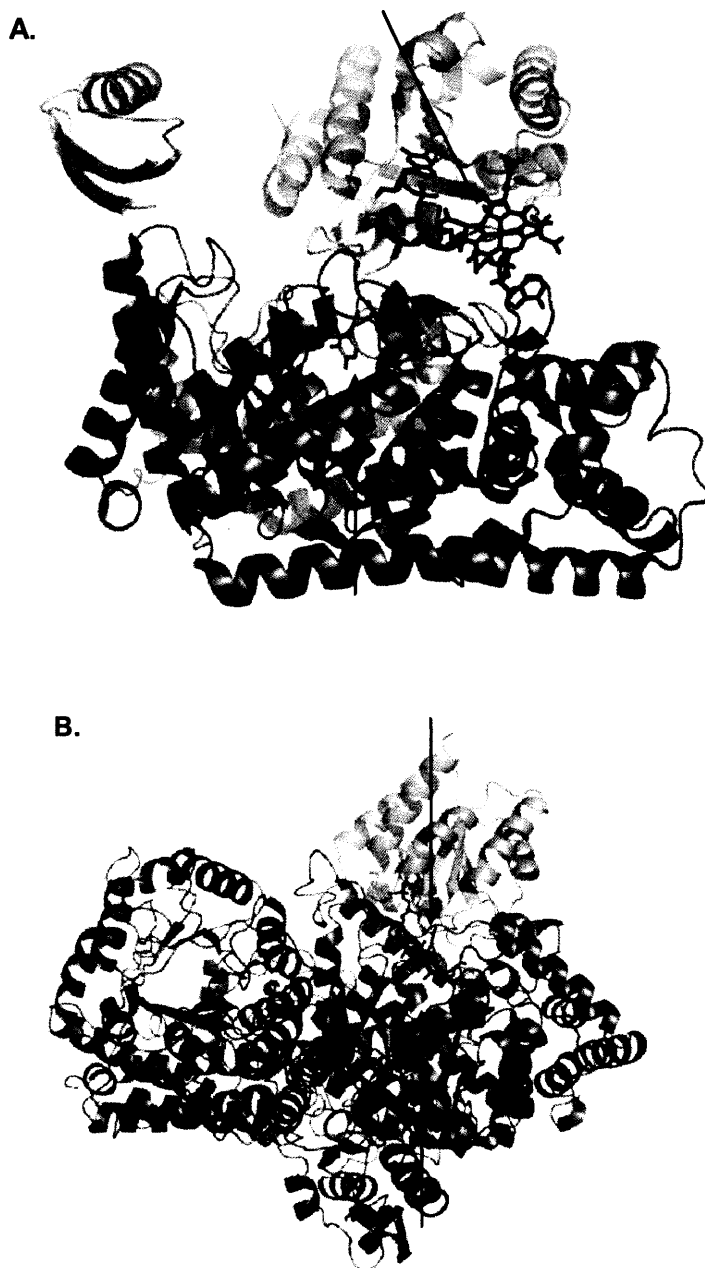
Figure 2.4. A. The structure of 5,6-LAM in its resting form, with AdoCbl 25 angstroms away from the active site *(1)*. B. A substrate-bound structure of Methylmalonyl coenzyme A mutase (Protein Data Bank ID code 1REQ), another enzyme that catalyzes radical chemistry with AdoCbl, with the AdoCbl positioned over the active site, in place for catalysis.
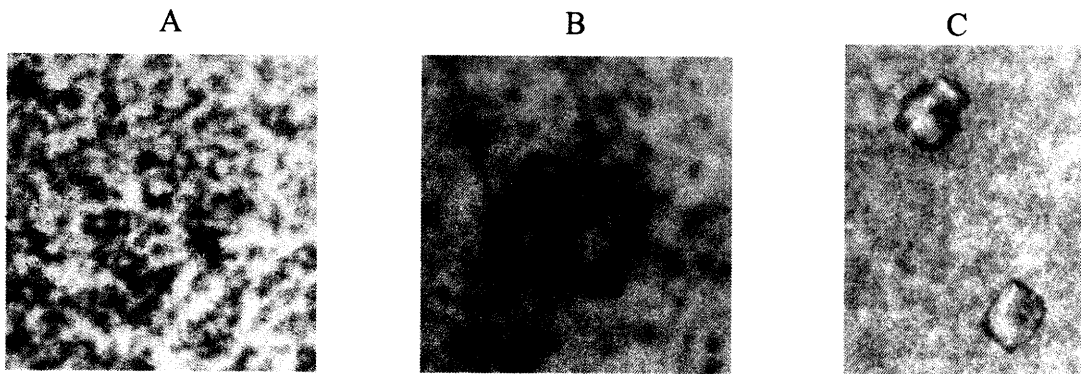
Figure 2.5. A. Original wt 5,6 LAM + 5mM lysine crystals (~15μm). B. Wild type 5,6 LAM + 5mM ornithine crystals (~50μm). C. 5,6-LAM K144βA mutant crystals (~50μm).
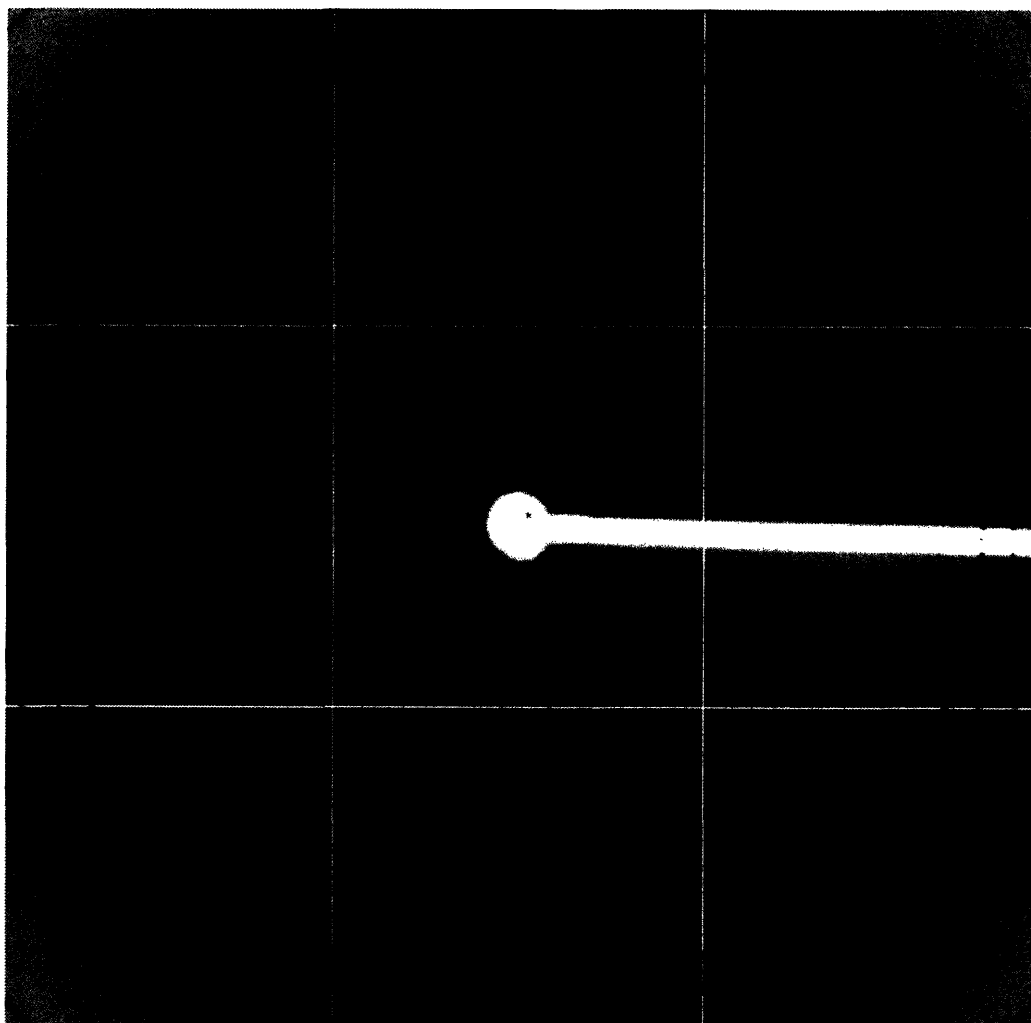
Figure 2.6. Diffraction Pattern from crystals of 5,6-LAM with 5mM ornithine from SSRL.
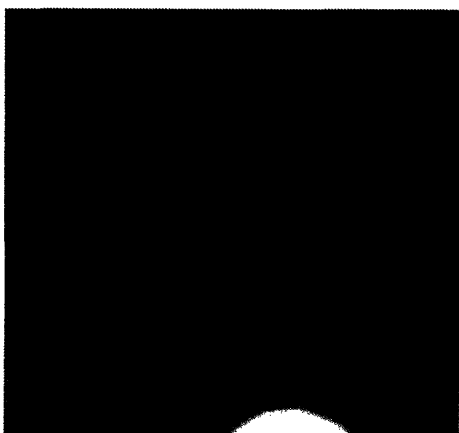
Figure 2.7. Close-up of spots from above diffraction pattern.
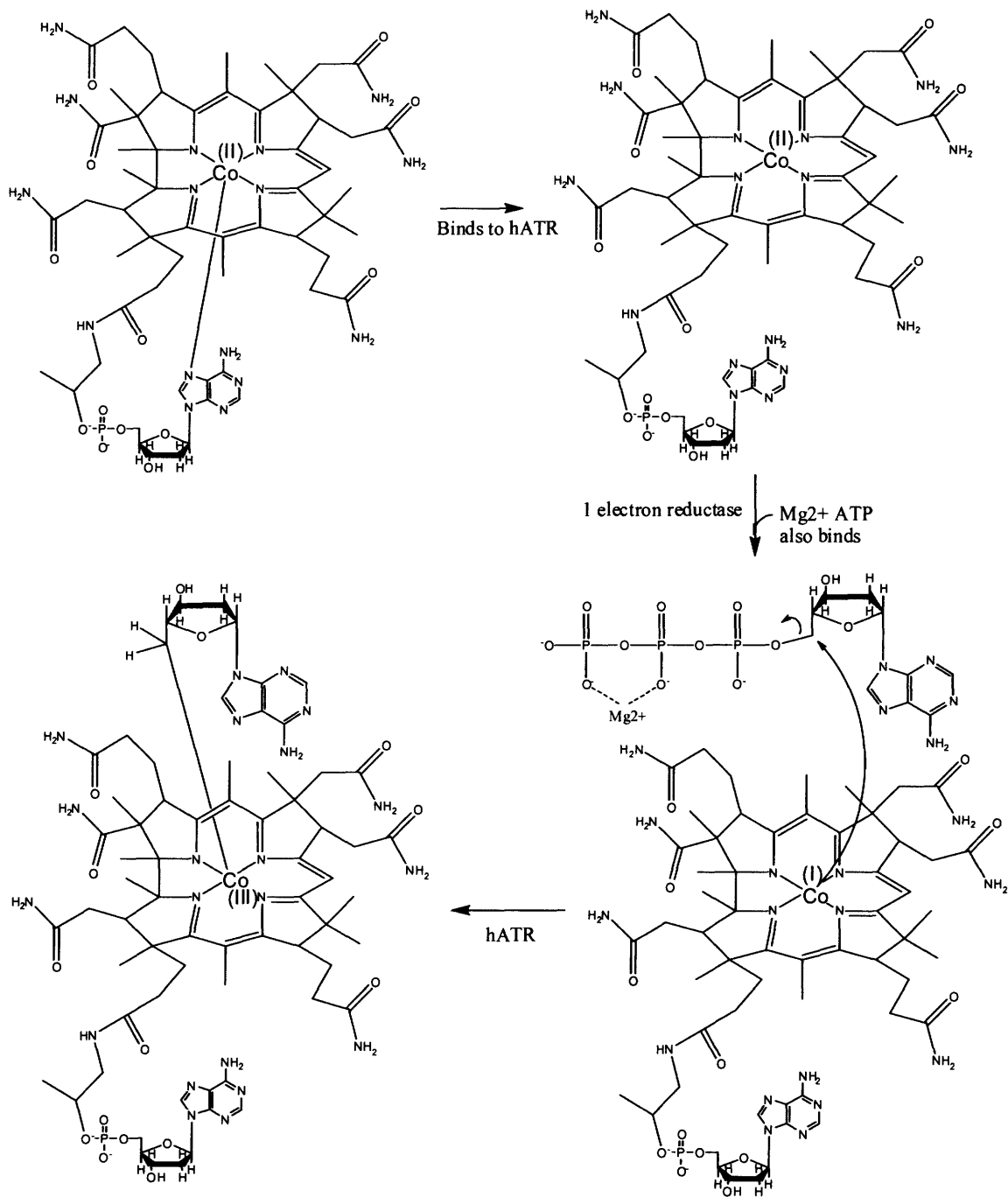
Figure 2.8. The reaction catalyzed by Adenosyltransferase *(27)*. The identity of the reductase is still unknown.
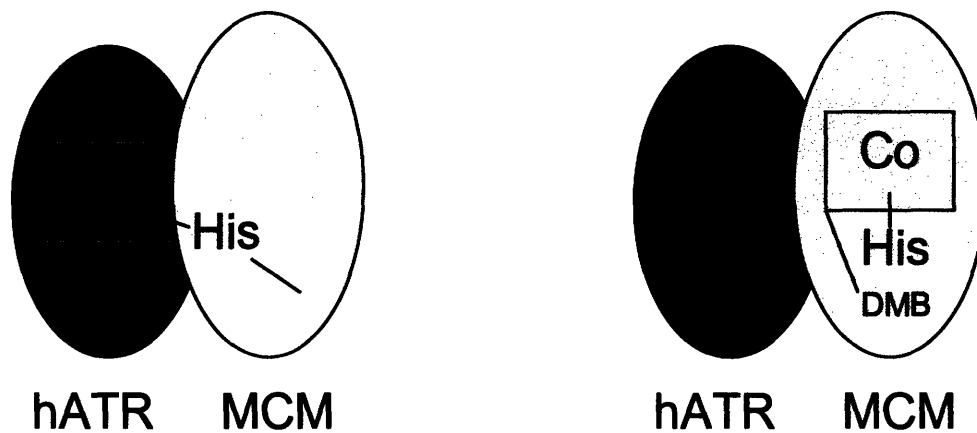
Figure 2.9. Representation of the proposed hand-off from hATR to MCM *(27)*.
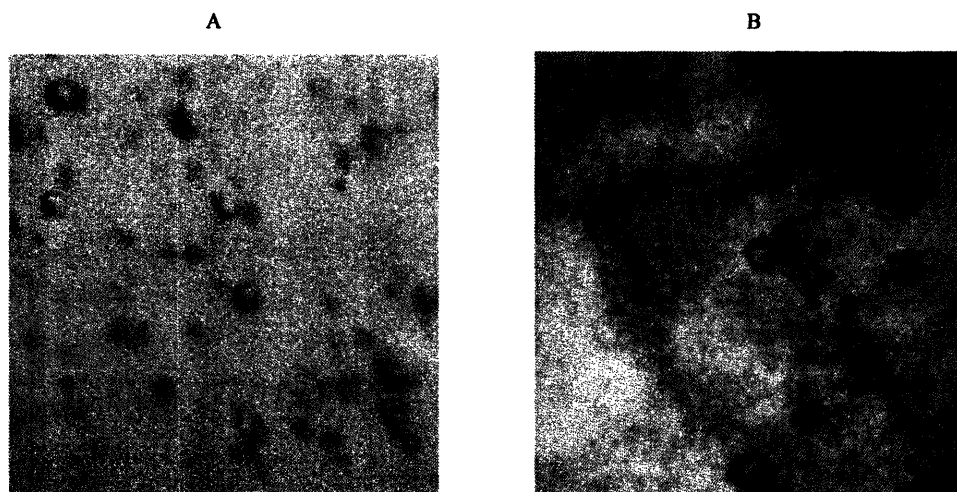
Figure 2.10. A. Preliminary crystals of hATR. B. Optimized crystals of hATR (30 μm).
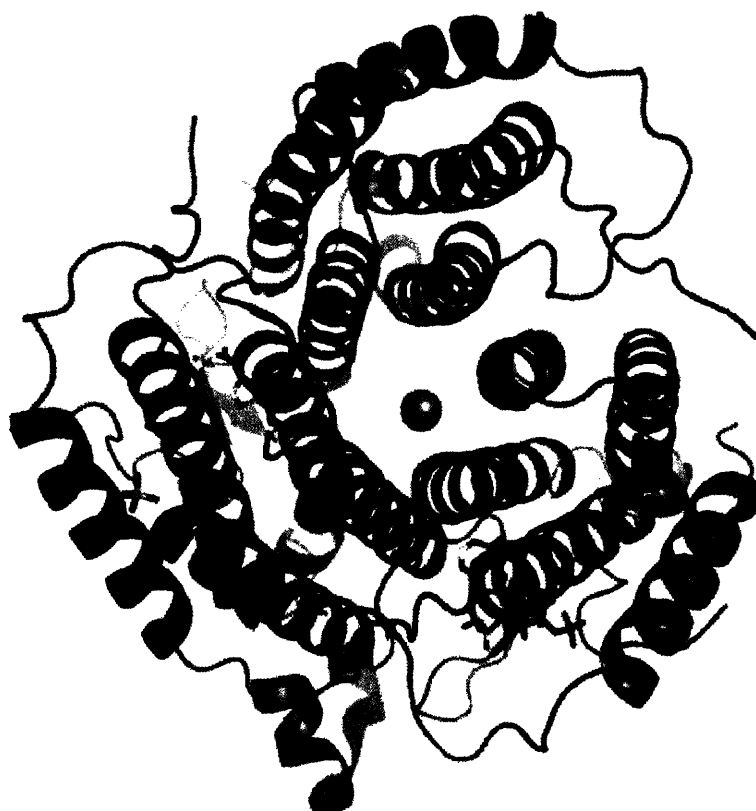
Figure 2.11. Crystal structure of hATR with ATP bound. hATR crystallized as a trimer with chloride bound in the middle *(32)*.

2.5. Tables

Screen	Hits	Screened Around	Result
Index	#81: 0.2 M Ammonium Acetate, 0.1M Tris pH=8.5, 25% w/v PEG 3350	Salt Salt Concentration Buffer/pH PEG Molecular Weight PEG Percentage Drop Size Protein Concentration Protein Buffer PLP Concentration Detergent Screens Additive Screens Detergent Concentration Additive Concentration Seeding	Optimized condition: 0.1M Hepes pH=8.2, 0.2M NH4OAc, 25% w/v PEG 2000MME with streak seeds No diffraction
Crystal Screen (20 mg/mL and 10 mg/mL protein)	None		
Crystal Screen #2 (20 mg/mL and 10 mg/mL protein)	None		
Crystal Screen Lite (10 mg/mL protein)	None		
Peg/Ion (15 mg/mL)	None		
MembFac (15 mg/mL)	None		
Natrix (15 mg/mL)	None		

Table 2.1. Crystallization trials of 5,6-LAM K144βA.

Screen	Hits	Screened Around	Result
Index with 5mM ornithine and 5mM lysine	#59 in drops with both ornithine and lysine: 22% Polyacrylic Acid, 0.1M Hepes pH=7.5, 0.02M MgCl$_2$	Buffer/pH Salt Salt Concentration Precipitant Precipitant Concentration Detergent Screens Additive Screens Protein Buffer Ornithine or Lysine Concentration B$_{12}$ Analog	Crystals grew, no diffraction
Crystal Screen with 5mM 6-aminohexanoate, ornithine and lysine	None		
Crystal Screen #2 with 5mM 6-aminohexanoate, ornithine and lysine	None		
Crystal Screen Lite with 5mM ornithine and lysine	None		
Peg/Ion	None		

Table 2.2. Crystallization trials of wild type 5,6-LAM with inhibitors added.

42

Screen	Hits	Screened Around	Result
Index	#77: 0.2 M LiSO4, 0.1 M Tris 8.5, 25% PEG 3350	PEG Percentage PEG Molecular Weight	No reproduction
	#84: 0.2 MgCl$_2$, 0.1 M Hepes pH=7.5, 25% PEG 3350	PEG Molecular Weight PEG Percentage Buffer/pH Salt Salt Concentration Detergent Screens Additive Screens	Nice, small crystals with PEG 2000 MME
	#85: 0.2 MgCl$_2$, 0.1 M Tris pH=8.5, 25% PEG 3350	PEG Molecular Weight PEG Percentage Buffer/pH Salt Salt Concentration Detergent screens Additive screens	Nice, small crystals with PEG 2000 MME
Crystal Screen	None		
Crystal Screen #2	#5 crystals (w/ ATP, no B$_{12}$). 2.0M (NH$_4$)$_2$SO$_4$, 5% isopropanol		Reproduced small crystals
Crystal Screen Lite	None		
Peg/Ion		Salt Salt Concentration PEG Concentration PEG Molecular Weight Buffer/pH	
Wizard I	None		
Wizard II	#19 interesting (w/ATP, no B$_{12}$): 1.6 M NaH$_2$PO$_4$/ 0.4M K$_2$HPO$_4$, 0.1 M Phosphate-Citrate buffer pH=4.2	Salt Concentration	Reproduced small crystals
MembFac	None		
Natrix	None		

Table 2.3. Crystallization trials of hATR (screens performed on all samples; hits only for without cobalamin).

2.6. References

1. Sintchak MD, Arjara G, Kellogg BA, Stubbe J, and Drennan CL. (2002) *Nat Struct Biol.* 9, 293-300.
2. Berkovitch F, Behshad E, Tang KH, Enns EA, Frey PA, & Drennan CL. (2004) *Proc Natl Acad Sci.* 101, 15870–15875.
3. .Reitzer R, Gruber K, Jogl G, Wagner UG, Bothe H, Buckel W, and Kratky, G. (1999) *Structure* 7, 891–902.
4. Mancia F, Keep NH, Nakagawa A, Leadlay PF, McSweeney S, Rasmussen B, Bosecke P, Diat O, and Evans PR. (1996) *Structure* 4, 339–350.
5. Sun L, Warncke K. (2006) *Proteins.* 64, 308-19.
6. Liao DI, Dotson G, Turner I Jr, Reiss L, and Emptage M. (2003*) J Inorg Biochem.* 93, 84-91.
7. Shibata N, Masuda J, Tobimatsu T, Toraya T, Suto K, Morimoto Y, and Yasuoka N. (1999) *Structure.* 7, 997-1008.
8. Wetmore SD, Smith DM, and Radom L. (2004) *J. Am. Chem. Soc.* 123, 8678-8689.
9. Danen WC and West CT. (1973) *J. Am. Chem. Soc.* 96, 2447–2453.
10. Chirpich TP, Zappia V, Costilow RN, Barker HA. (1966) *J Biol Chem.* 245, 1778-1789.
11. Chang CH, and Frey PA. (2000) *J. Biol. Chem.* 275, 106–114.
12. Tang KH, Casarez AD, Wu W, and Frey PA. (2003) *Arch. Biochem. Biophys.* 418, 49–54.
13. Baker JJ, van der Drift C, and Stadtman TC. (1973) *Biochemistry* 12, 1054-1063.
14. Tang KH, Chang CH, and Frey PA. (2001) *Biochemistry* 40, 5190–5199.
15. Finney LA and O'Halloran TV. (2003) *Science* 300, 931-936.
16. Rosenblatt DS, *et. al.* (1984) *J. Clin. Invest.* 74, 2149-2156.
17. Shevell MA and Rosenblatt DS. (1992) *Can. J. Neuro. Sci.* 19, 472-486.
18. Dobson CM, *et. al.* (2002) *Hum. Mol. Genet.* 11, 3361-3369.
19. Lerner-Ellis JB, *et. al.* (2006) *Mol. Genet. Metab.* 87, 219-225.
20. Johnson CL, *et. al.* (2001) *J. Bacteriol.* 183, 1577-1584.
21. Suh S, and Escalante-Semerana JC. (1995) *J. Bacteriol.* 177, 921-925.
22. Buan, N.R., *et. al.* (2004) *J. Bacteriol.* 186, 5708-5714.
23. Brown KL and Hakimi JM. (1984) *J. Am. Chem. Soc.* 106, 7894-7899.
24. Drennan CL, Huang S, Drummond JT, Matthews RG, and Ludwig ML. (1994) *Science.* 266, 1669-74.
25. Bauer CB, *et. al.* (2001) *Biochemistry* 40, 361-374.
26. Saridakis V, *et. al.* (2004) *J. Biol. Chem.* 279, 23646-23653.
27. Yamanishi M, *et. al.* (2005) *TRENDS in Biochem. Sci.* 30, 304-308.
28. Lexa D and Saveant JM. (1983) *Acc. Chem. Res.* 16, 235-243.
29. Yamanishi M, *et. al.* (2005) *J. Am. Chem. Soc.* 127, 526-527.
30. Stich TA, *et. al.* (2005) *J. Am. Chem. Soc.* 127, 7660-7661.
31. Pufahl RA, *et. al.* (1997) *Science* 278, 853-856.
32. Schubert HL and Hill CP. (2006) *Biochemistry.* 45, 15188-96.
33. St Maurice M, Mera PE, Taranto MP, Sesma F, Escalante-Semerena JC, Rayment I. (2007) *J Biol Chem.* 282, 2596-605.
34. Tang KH, Harms A, Frey PA. (2002) *Biochemistry.* 27, 8767-76.

3. Lipoate synthase and class III ribonucleotide reductase activating enzyme crystallization studies

3.1. Introduction to crystallography of *S*-adenosylmethionine radical enzymes

The structures of four *S*-adenosylmethionine (AdoMet) radical enzymes have been solved to date *(1,2,3,4)*. All of them show the active site in a full *(1)* or three-quarter *(2,3,4)* TIM barrel. It has been proposed that this difference in barrel completeness could be due to different enzymes needing to accommodate substrates varying greatly in size *(5)*. All crystallized enzymes have the catalytically essential [4Fe-4S] cluster in the structure, and biotin synthase (BioB) also has an additional [2Fe-2S] cluster, positioned to be the sulfur donor in the sulfur-insertion reaction *(1)*. Crystallization of this family of enzymes has been very difficult, possibly due to protein preparations not having full occupancy of the [4Fe-4S] site and the need for strict anaerobosis.

3.2. Lipoate synthase

3.2.1. Introduction

Lipoate synthase (LipA) is an AdoMet radical enzyme that catalyzes 2 sulfur insertions to make the lipoyl cofactor from an octanoyl group (Figure 3.1). The lipoyl cofactor is used in several enzyme complexes, most notably the pyruvate dehydrogenase complex, which is essential for aerobic metabolism. It functions as both a redox cofactor and as a "swinging arm," allowing the attached substrate to go from one subunit to another tethered to the lipoyl cofactor, which is covalently bound to a lysine residue on enzyme E2.

LipA follows the general AdoMet radical enzyme mechanism of 5'-deoxyadenosyl radical (Ado•) generation. This proposed mechanism consists of the reduction of the catalytically essential [4Fe-4S] cluster to $[4Fe-4S]^{1+}$ from $[4Fe-4S]^{2+}$, followed by the injection of this electron into the sulfur of AdoMet. AdoMet is then reductively cleaved to form methionine and Ado• . In the case of LipA, the Ado• is then proposed to abstract a hydrogen atom from either C-6 or C-8 of the octanoyl group, allowing for subsequent sulfur insertion (6). This radical-based mechanism is supported by experiments performed in Squire Booker's laboratory in which a deuterium atom on the octanoyl group is transferred to 5'-deoxyadenosine during catalysis (6). In addition, two molar equivalents of AdoMet are used to form one mole of lipoic acid, consistent with the idea of one Ado• abstracting a hydrogen atom from C-6, and one Ado• abstracting a hydrogen atom from C-8 (6). This reaction is analogous to that performed by BioB, another AdoMet radical enzyme, which catalyzes the insertion of one sulfur into two unactivated carbon-hydrogen bonds (Figure 3.1).

In addition to the [4Fe-4S] cluster present in all AdoMet radical enzymes, LipA also contains a second [4Fe-4S] cluster (7). Similarly, the other sulfur-insertion AdoMet radical enzyme, biotin synthase (BioB) contains a second cluster, but in that case it is a [2Fe-2S] cluster. While debated for some time, it is now widely accepted that the sulfur that is inserted into dethiobiotin comes from this [2Fe-2S] cluster. This proposal is supported by the structure (1), which shows this cluster in close proximity to dethiobiotin, as well as by ^{34}S labeling studies (8) and experiments which show the

destruction of the [2Fe-2S] cluster that accompanies biotin formation *(9,10)*. BioB has

only ever shown one turnover *in vitro (11,12,13)*, which is consistent with the cluster

being the sulfur source; however, multiple turnovers were seen *in vivo (14)*, suggesting

the rebuilding of the cluster or a different sulfur source *in vivo*. So far, no proteins have

been identified that rebuild the [2Fe-2S] cluster of BioB *in vitro* or *in vivo* and no other

sulfur sources have been identified. In the case of LipA, there is no clear evidence for

destruction of the second [4Fe-4S] cluster *(7)*.

An X-ray structure of LipA could provide important information about the source of

sulfur and mechanism of sulfur insertion. Until recently, no one had seen LipA turnover

at all *in vitro*. Work from the laboratories of Marletta and Cronan have established the

substrate for LipA as octanoic acid bound to the E2 subunit of the pyruvate

dehydrogenase, as opposed to free octanoic acid or octanoyl-ACP (*15*), and work from

Squire Booker's laboratory has shown that the octanoylated H-protein of the glycine

cleavage system, another lipoyl-bearing enzyme subunit, can also be a LipA substrate *(6)*.

This work allowed lipoic acid to be produced *in vitro*; however, multiple turnovers have

not been seen.

Since the reactions catalyzed by BioB and LipA are so similar (Figure 3.1), a structural

comparison of these enzymes would provide significant insight into sulfur insertion

chemistry by AdoMet radical enzymes. One aspect of the structure that would be

particularly informative is the placement of the second iron-sulfur cluster with respect to

the substrate. If the cluster is far away from the substrate, its role as a sulfur source

would be unlikely. If it is close to the substrate, it could potentially be the sulfur source, or be involved in sulfur insertion without being the final sulfur source.

3.2.2. Previous work in the Booker laboratory

Recent work in the laboratory of Prof. Squire Booker at Pennsylvania State University has focused on obtaining pure, homogeneous, and active LipA with improved stability (S. Booker, personal communication). Stable protein can now be obtained in high enough yields for crystallization experiments (S. Booker, personal communication). The identification of the true substrate has made it possible to assay the protein during purification (15). In addition, the discovery that LipA should have a complement of eight, not four, Fe's per monomer has led to more stable and homogeneous protein samples (7).

3.2.3. Crystallization experiments

Sparse matrix screens (Table 3.1) with degassed solutions in a Coy anaerobic chamber at room temperature have been used to screen fully reconstituted LipA (8 Fe's per monomer), LipA with AdoMet, LipA with octanoylated H-protein, and LipA with AdoMet and octanoylated H-protein, all obtained from the Booker laboratory. The protein was at 8 mg/mL in 50 mM Epps buffer, pH 8.0, 100 mM KCl, 10 mM DTT, and 20% glycerol. AdoMet was added in a 2:1 ratio to LipA, and octanoylated H-protein in the same buffer as LipA was added in a 1:1 ratio. There were several potentially promising conditions that were screened around (Table 3.1). However, none of these conditions have been reproducible, and no amount of screening around these conditions

has resulted in anything crystalline. Multiple protein preparations obtained from the Booker laboratory have been screened, all with similar results. It is possible that the protein is highly sensitive to slight changes in humidity and temperature, and this is causing the lack of reproducibility; it is also possible that the small amount of oxygen that still exists in the anaerobic chamber is affecting crystallization.

3.2.4. Conclusions and future work

The Booker laboratory is working on expressing and purifying protein from a thermophilic organism. Due to the high temperatures in which these organisms grow, their proteins can be more stable, and can crystallize more easily. If crystals of LipA are obtained, the structure will be solved by native Fe-MAD techniques, which have been successful in our laboratory *(1)*. Subsequent structures of different forms of LipA will be determined by molecular replacement. This structural information should greatly enhance our understanding of how nature makes biotin and lipoic acid.

3.3. Class III ribonucleotide reductase activating enzyme

3.3.1. Introduction

Radical chemistry is believed to be ancient, with ribonucleotide reductases (RNRs) potentially providing the link between the RNA and DNA world. The common chemistry and active site structure of the three classes of RNRs suggest they evolved by divergent evolution, with class III RNR as the likely progenitor *(16)*. Since class I RNR requires oxygen for catalysis, it must have arisen after photosynthesis led to an O_2 atmosphere. Class II RNR uses AdoCbl, and does not need oxygen, but can work in an oxygen atmosphere. Class III RNR, with an AdoMet radical enzyme activase, requires anaerobic conditions for catalysis. Class III RNR's use of formate as a reductant instead of a several-protein electron transport chain is a strong argument in favor of the Class III enzyme being the first RNR; also, it is thought that AdoMet could be the evolutionary forerunner of AdoCbl, since it is easier to synthesize and can perform a similar function. The class III RNR activating enzyme (NrdG, also known as the beta protein) abstracts a hydrogen atom from the catalytic subunit of class III RNR (the alpha protein), forming a stable glycyl radical. This glycyl radical can then abstract a hydrogen atom from a cysteine to form a transient thiyl radical which initiates catalysis, resulting in a nucleotide being reduced to a deoxynucleotide and formate being oxidized to carbon dioxide (Figure 3.2) *(Reviewed in 17)*.

NrdG is the simplest AdoMet radical enzyme by sequence alignment *(6)*. NrdGs only have about 160 amino acids, which is too short for a full $(\alpha\beta)_8$ or a three-quarters $(\alpha\beta)_6$ TIM barrel. Sequence similarities between NrdG and other AdoMet radical proteins ends

at helix α_4, suggesting that it might contain a half $(\alpha\beta)_4$ TIM barrel. While it's possible from the alignment that it could have strand 5, it is missing a GxIxGxxE-like sequence usually at the end of strand 5 to that binds AdoMet in other AdoMet radical enzymes (5). In the structures of AdoMet radical enzymes that have been solved, AdoMet binds to residues on strands 5 and 6 of the barrel; therefore, if NrdG has a half-barrel structure, the manner of AdoMet binding must differ significantly from that of the currently available structures of AdoMet enzymes.

According to sequence alignment, NrdG does not have the helix α_{4A} usually present in TIM barrels (5). Thus, helix α_4 may be on the inner side of the β-sheet, close to the substrate, instead of on the other side of the sheet (5). If this is the case, the helix could help bind AdoMet, potentially compensating for the absence of sheets 5 and 6 (5). It has been suggested that $(\alpha\beta)_4$ half-barrels would have a tendency to aggregate, and would have had to evolve an extra half-barrel or another strand and helices to cover up the exposed beta sheet (18). Purified alone, NrdG is prone to aggregation, supporting the half-barrel hypothesis (19). Since NrdG has a protein as its substrate, perhaps removing the tendency to aggregate by evolving a full barrel would not allow for substrate access to the active site, explaining why NrdG kept the half barrel. The reason NrdG does not aggregate *in vivo* is probably related to increased stability due to dimerization or association with its substrate, the class III RNR catalytic subunit (5). In fact, it is impossible to separate the *E. coli* catalytic subunit and activase by chromatography (19), and it is known to dimerize *in vivo* (19).

A structure of NrdG would shed light on the evolution of TIM barrels in AdoMet radical enzymes. TIM barrels used for AdoMet radical chemistry are believed to have evolved either by gene duplication from half barrels followed by subsequent evolution of the C-terminal sequence to accommodate a wide range of substrates and reactivities, while conserving the radical generation function with the $(\alpha\beta)_6$ subdomain, or from adding $(\alpha\beta)_2$ units to the $(\alpha\beta)_4$ core unit *(5)*. The structure of NrdG would be important to distinguish between these theories. The NrdG complex structure would show how AdoMet radical enzymes have evolved to accommodate huge differences in substrate size, as well as reveal the simplest model for AdoMet radical catalysis.

3.3.2. Previous work in the Fontecave laboratory

The Fontecave laboratory has been able to produce large amounts of pure protein of the alpha/beta complex. They have identified both flavodoxin *(20)* and thioredoxin *(21)* as potential sources of the electron that reduces the cluster from $[4Fe-4S]^{2+}$ to $[4Fe-4S]^{1+}$ in *E. coli* and confirmed that this reduced cluster is necessary for the reaction to proceed.

3.3.3. Crystallization experiments

Sparse matrix screens with degassed solutions in a Coy anaerobic chamber at room temperature have been used to screen the protein samples (Table 3.2). The first sample was of the alpha/beta complex prepared by adding the alpha protein to the just-reconstituted beta protein in a 1:1 molar ratio at a final concentration of 40 mg/mL and then adding 2.5 mM enantiomerically pure AdoMet. The second sample was of the complex alpha/beta prepared by adding the alpha protein to the newly reconstituted beta

protein in a 1:1 molar ratio, also giving a final concentration of 40 mg/mL, and then adding 2.5 mM AdoMet. The third sample of the complex alpha/beta was prepared by adding an equimolar amount of the alpha protein to the newly reconstituted beta protein to give a final protein concentration of 40 mg/mL in the presence of 2.5 mM purified AdoMet and 5mM ATP. All of the samples were in 10 mM Tris-HCl, pH 7.5, and 2 mM DTT. The sparse-matrix crystallization screens were performed at both 3 mg/mL and 6 mg/mL. One condition was interesting enough to screen around, but no crystals formed (Table 3.2). Most of the drops contained heavy precipitate, even at 3 mg/mL.

3.3.4. Conclusions and future work

At this point, solving the crystal structure of the alpha/beta complex does not seem promising. Given the heavy precipitation of the protein at low concentrations, it appears as though the protein is denaturing in most every drop; perhaps ongoing work in the Fontecave laboratory identifying mutants of both proteins that are more stable will yield crystals of the complex. If crystals are grown, the structure could be solved either with molecular replacement using the known structure of the alpha protein homolog, or with Fe MAD techniques.

3.4. Figures
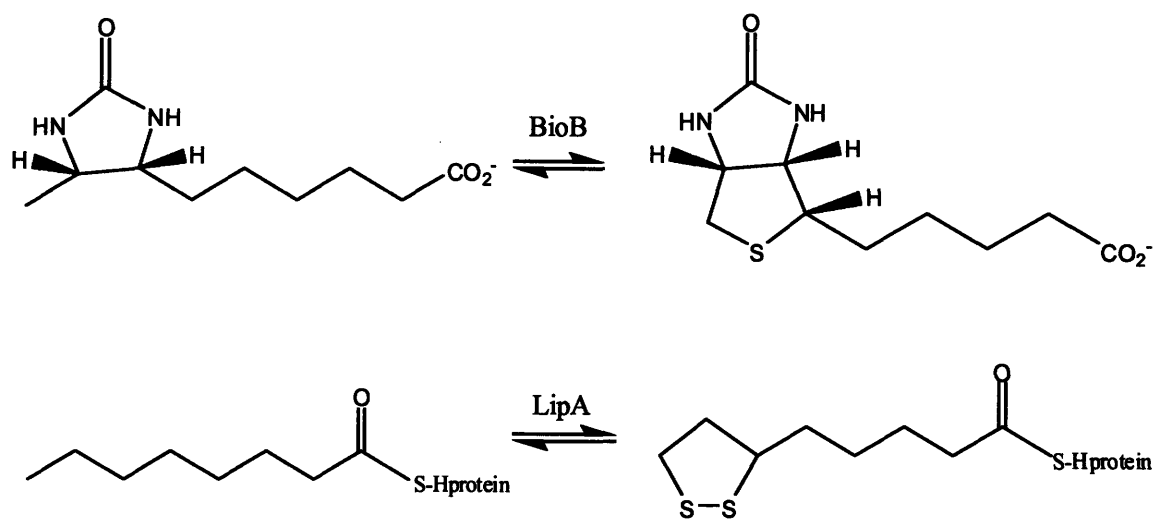
Figure 3.1: BioB and LipA use radical-based chemistry to catalyze sulfur insertion reactions.
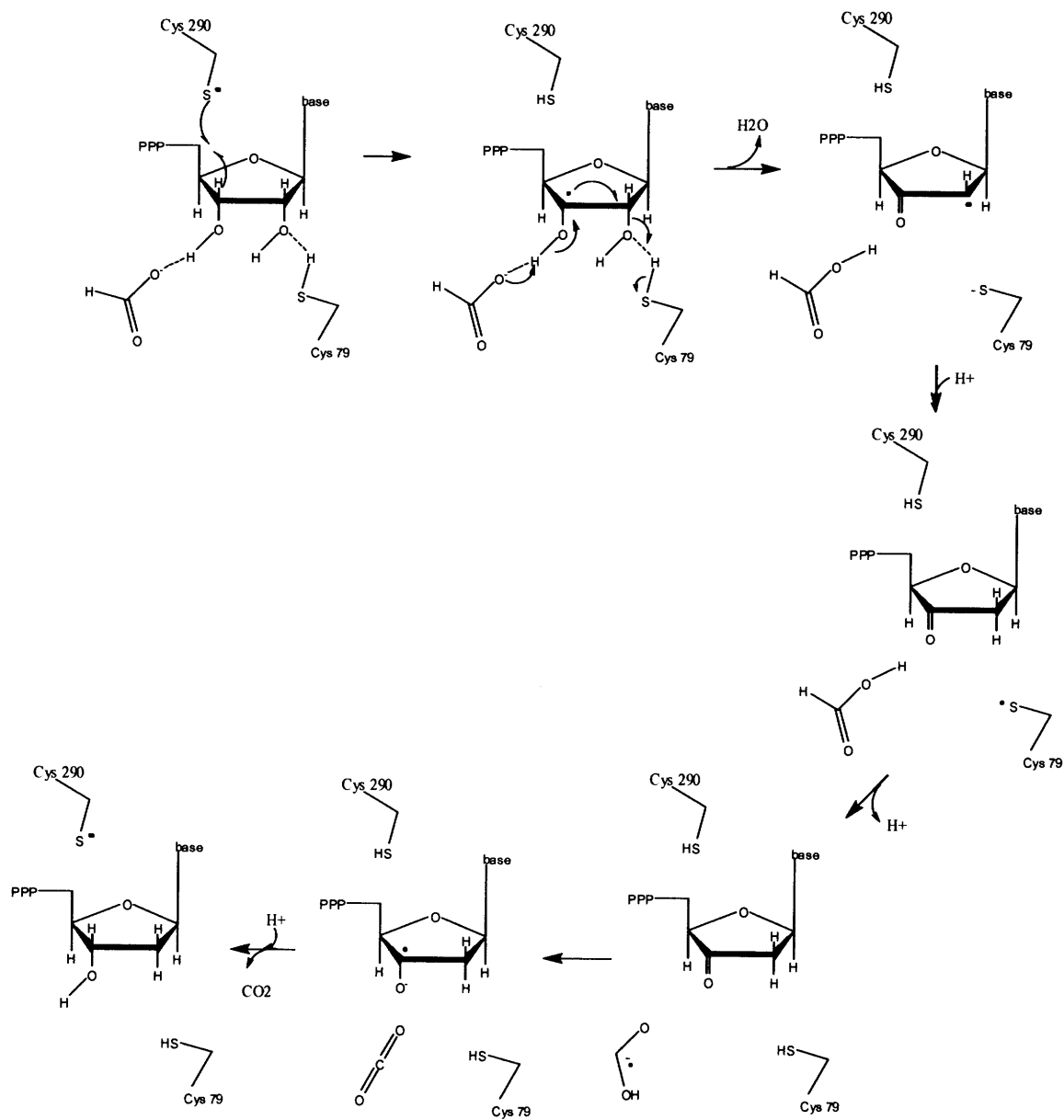
Figure 3.2. Mechanism of class III RNR *(17)*.

3.5. Tables

Screen	Hits	Screened Around	Result
Index	#62: 0.2 M trimethylamine N-oxide, 0.1 M Tris pH=8.5, 20% PEG 2000 MME	Buffer/pH PEG Concentration Salt Concentration	No reproduction
	#69: 0.2 M Ammonium Sulfate, 0.1 M Tris pH=8.5, 25% PEG 3350 MME	Buffer/pH PEG Concentration Salt Concentration	No reproduction
Crystal Screen	None		
Crystal Screen #2	None		
Crystal Screen Lite	None		
Peg/Ion	#1: 0.2 M NaF, 20% w/v PEG 3350	Salt Salt Concentration PEG Concentration PEG Molecular Weight	No reproduction
	#10: 0.2 M NaI, 20% w/v PEG 3350	Salt Salt Concentration PEG Concentration PEG Molecular Weight	No reproduction
	#11: 0.2 M KI, 20% w/v PEG 3350	Salt Salt Concentration PEG Concentration PEG Molecular Weight	No reproduction
	#27: 0.2 M Sodium Acetate, 20% w/v PEG 3350	Salt Salt Concentration PEG Concentration PEG Molecular Weight	No reproduction
Wizard I	None		
Wizard II	None		
Pro-Complex	None		

Table 3.1. Crystallization screening of LipA (all samples).

Screen	Hits	Screened Around	Result
Index	None		
Crystal Screen	None		
Crystal Screen #2	None		
Crystal Screen Lite	None		
Peg/Ion	#12: 0.2M Ammonium Iodide, 20% PEG 3350	Salt Salt Concentration PEG Concentration PEG Molecular Weight Buffer/pH	No reproduction
Wizard I	None		
Wizard II	None		
Pro-Complex	None		

Table 3.2. Screening of class III RNR complex (all samples).

3.6. References

1. Berkovitch F, Nicolet Y, Wan JT, Jarrett JT, and Drennan CL. (2004) *Science* 303, 76-79.
2. Hanzelmann P and Schindelin H. (2004) *Proc Natl Acad Sci* 101, 12870-5.
3. Layer G, Moser J, Heinz DW, Jahn D, and Schubert WD. (2003) *EMBO J.* 22, 6214-24.
4. Lepore BW, Ruzicka FJ, Frey PA, and Ringe D. (2005) *Proc Natl Acad Sci* 102, 13819-24.
5. Nicolet Y and Drennan C. (2004) *Nucleic Acids Res.* 32, 4015-4025.
6. Cicchillo RM, Iwig DF, Jones AD, Nesbitt NM, Baleanu-Gogonea C, Souder MG, Tu L, and Booker SJ. (2004) *Biochemistry* 43, 6378-6386.
7. Cicchillo RM and Booker SJ. (2005) *J Am Chem Soc.* 127, 2860-2861.
8. Tse Sum Bui B, Florentin D, Fournier F, Ploux O, Mejean A, and Marquet A. (1998). *FEBS Lett.* 440, 226-230.
9. Ugulava NB, Sacanell CJ, and Jarrett JT. (2001) *Biochemistry* 40, 8352-8358.
10. Tse Sum Bui B, Florentin D, Marquet A, Benda R, and Trautwein AX. (2003) *Biochemistry* 42, 8791-8798.
11. Ollagnier-de Choudens S, Mulliez E, Hewiston KS, and Fontecave M. (2002) *Biochemistry* 41, 9145-9152.
12. Sanyal I, Cohen G, and Flint DH. (1994) *Biochemistry* 33, 3625-3631.
13. Ugulava NB, Gibney BR, and Jarrett JT. (2001) *Biochemistry* 40, 8343-8351.
14. Zhao X, Miller JR, Jiang Y, Marletta MA, and Cronan JE. (2003) *Chem. & Biol.* 10, 1293-1302.
15. Cicchillo RM, Lee K, Baleanu-Gogonea C, Nesbitt NM, Krebs C, and Booker SJ. (2004) *Biochemistry* 43, 11770-11781.
16. Reichard P. (1997) *Trends Biochem Sci.* 3, 81-5.
17. Kolberg M, Strand KR, Graff P, and Andersson KK. (2004) *Biochim Biophys Acta.* 1699, 1-34.
18. Hocker B, Schmidt S, and Sterner R. (2002) *FEBS Lett* 510, 133-135.
19. Fontecave M, Mulliez E, and Logan DT. (2002) *Prog. Nucleic Acid Res. Mol. Biol.* 72, 95-127.
20. Mulliez E, Padovani D, Atta M, Alcouffe C, and Fontecave M (2001) *Biochemistry.* 40, 3730-6.
21. Padovani D, Mulliez E, and Fontecave M. (2001) *J Biol Chem.* 276, 9587-9.

Appendix 1
Protein expression, purification, and crystallization trials of *O*-GlcNAC transferase

O-GlcNAC Transferase catalyzes the transfer of *N*-acetylglucosamine from UDP-GlcNAC to serine and threonine residues of proteins important in eukaryotic signaling. The glycosylation state of these target proteins is key to signaling cascades involved in glycose homeostasis and stress response *(1)*. My collaborator in the Walker lab has developed a protein prep method that allows isolation of large amounts of pure sOGT of truncation mutants and splice variants *(2)*. He used this protein to test for inhibitors *in vitro* (2) and to try crystallizing the protein with a crystallization robot, but no crystals were formed (Ben Gross, personal communication).

Protein Prep with Ben (sOGT)—
1. Lysed cells with 50 uL Lyonase in 400mL Bug Buster
2. Centrifuged 25 minutes at max rpm
3. Prepped Ni-ITA column, put protein on column at 2 mL/min flow rate
4. Used 50mM Imidazole, 250 mM NaCl, pH=7.6 to wash until Bradford reagent light colored
5. Eluted with 200mM imidazole 250 mM NaCl pH=7.6 until Bradford reagent light colored.
6. Combined fractions eluted at 200mM imidazole, concentrated
7. Injected half of protein through through FPLC, using Superdex 200 Column and 10mM imidazole, 250mM NaCl, 1mM EDTA pH=6. There were only 2 peaks, a void peak and a protein peak. The protein peak eluted from 70-90 minutes.
8. Cut off his-tag with HRV3C overnight with other half of protein
9. Injected other half through FPLC.
10. Concentrated both portions of protein, did buffer exchange into 10mM imidazole pH=7.6, 1mM EDTA.
11. Found concentration of 1 mL of OGT + His-tag to be 5.63 mg/mL
12. Found concentration of 1 mL of OGT − His-tag to be 16.68 mg/mL.
13. Gel of both looked relatively clean.

Crystallization Trials:

Screen	Hits	Screened Around	Result
Index (Straight)	None		
Index (diluted 2x)	#22 diluted 2x: 0.8 M Succinic Acid pH 7.0.	pH Succinic Acid Concentration	Very tiny crystals reproduced, didn't grow
Index (diluted 2x) (with 4 inhibitors, each 1 μM)	None		
Crystal Screen (diluted 2x)	None		
Crystal Screen #2 (diluted 2x)	#1 interesting, diluted 2x: 0.5 M CoCl₂, 0.05 M NaOAc pH=4.6, 0.5M Hexanediol	Salt Concentration Precipitant Concentration	Nothing Interesting
Crystal Screen Lite	None		
Peg/Ion (diluted 2x)	None		
Wizard I (diluted 2x)	#33 diluted 2x: 1.0M (NH₄)₂SO₄, 0.05M CAPS pH=10.5, 0.1M Li₂SO₄.	Salt Concentrations	No reproduction
Wizard II (diluted 2x)			
Wizard III (diluted 2x)			
Pro-Complex (diluted 2x)			
Salt Rx (diluted 2x)	#46 diluted 2x: 2.0M NaNitrate, 0.05M NaOAc pH=4.6.	Buffer/pH Salt Concentration	No reproduction
Salt Rx (diluted 2x) (with 4 inhibitors, each 1 μM)	#10 diluted 2x: 1.1 M NaCl, 0.05M Bis-Tris propane 7.0	NaCl Concentration	No reproduction
NaCl Grid Screen (diluted 2x) (with 1 inhibitor, 1 μM)	None		
MembFac (diluted 2x)	None		
Natrix (diluted 2x)	None		
Ammonium Sulfate Grid Screen (with 4 inhibitors, each 1 μM)	#15 with 1 inhibitor: 2.4 M Ammonium Sulfate, 0.1M MES pH 6.0.	Salt Concentration Detergent Screens Additive Screens Seeding	No optimization—very small crystals

Tried performing protein expression and preparation of stock cells from all four cell lines sent from Ben—no expression for any of them.

Transformed cells with sOGT and ncOGT. No expression was seen for either construct.

1. Zachara NE, Hart GW. (2004) *Biochim. Biophys. Acta 1673*, 13-28.
2. Gross BJ, Kraybill BC, and Walker S. (2005) *J. Am. Chem. Soc.* 127, 14588 -14589.

Appendix 2
Curriculum Vitae   Laura Phillips

56-546   lauraphillips81@yahoo.com
77 Massachusetts Ave   (617) 721-0895
Cambridge, MA 02139

Education
Carleton College, 1999-2003
Graduated Magna Cum Laude with major in Chemistry, Concentration in Biochemistry
GPA 3.82 out of 4.0. Science GPA 3.91/4.0.

Massachusetts Institute of Technology, 2004-present
Graduate Student in Biological Chemistry
GPA 5.0/5.0.

Research Experience
University of Washington, Undergraduate research performing fluorescent telomere quantitation in the lab of Peter Rabinovitch in the Department of Pathology, 2001.

Carleton College, Researcher performing organic synthesis reactions and looking at ^{1}H/^{2}H exchange using ^{2}H NMR in the lab of Jerry Mohrig in the Chemistry Department, 2002-2003.

University of Minnesota, Lab Technician studying Nitrogen Mustard and Diepoxybutane reactivity with DNA bases in the lab of Natalia Tretyakova in the Medicinal Chemistry Department, 2003-2004.

Massachusetts Institute of Technology, Research Assistant working on X-ray crystallography of Metalloenzymes in the lab of Cathy Drennan, 2005-present.

Teaching Experience
Carleton College, Organic Chemistry TA, 2001-2002
Carleton College, Lab TA for advanced NMR lab, 2003
Massachusetts Institute of Technology, TA for Advanced NMR/EPR lab, 2004
Massachusetts Institute of Technology, TA for General Chemistry, 2 semesters, 2005
Mentor to an undergraduate research student in the Drennan Lab

Awards/Honors
Participant, Howard Hughes Undergraduate Research Program in the Biological Sciences, 2001
Carleton College Dean's List
Sigma Xi Member, Carleton College
Phi Beta Kappa Member, Carleton College
Cambridge Science Foundation Travel Grant, 2005

Conferences
The American Chemical Society Conference (2003), Poster Presentation
Gordon Research Conference on Vitamin B12 (2005), Poster Presentation

Fellowships
NIH Biotechnology Training Program Trainee, Awarded 2006
Martin Family Society of Fellows for Sustainability Member, Awarded 2006

Publication
Balcome, S., Park, S., Phillips, L., Hafner, L., Quirk Dorr, D., and Tretyakova, N.: Adenine-containing DNA-DNA cross-links of antitumor nitrogen mustards. *Chem Res Toxicol.* 2004 Jul;17(7)